Available online at www.sciencedirect.com
SCIENCE DIRECT®
Journal of Computational Physics 188 (2003) 16–55
JOURNAL OF COMPUTATIONAL PHYSICS
www.elsevier.com/locate/jcp

Construction of second order accurate monotone and stable residual distribution schemes for unsteady flow problems

Rémi Abgrall [*,1], Mohamed Mezine [2]

Mathématiques Appliquées de Bordeaux, Université Bordeaux I, 351 cours de la Libération, 33 405 Talence Cedex, France

Received 22 May 2002; received in revised form 15 October 2002; accepted 26 November 2002

Abstract

The aim of this paper is to construct upwind residual distribution schemes for the time accurate solution of hyperbolic conservation laws. To do so, we evaluate a space–time fluctuation based on a space–time approximation of the solution and develop new residual distribution schemes which are extensions of classical steady upwind residual distribution schemes. This method has been applied to the solution of scalar advection equation and to the solution of the compressible Euler equations both in two space dimensions. The first version of the scheme is shown to be, at least in its first order version, unconditionally energy stable and possibly conditionally monotonicity preserving. Using an idea of Csik et al. [Space–time residual distribution schemes for hyperbolic conservation laws, 15th AIAA Computational Fluid Dynamics Conference, Anahein, CA, USA, AIAA 2001-2617, June 2001], we modify the formulation to end up with a scheme that is unconditionally energy stable and unconditionally monotonicity preserving. Several numerical examples are shown to demonstrate the stability and accuracy of the method.

AMS: 65C99; 65M60; 76N10

Keywords: Compressible flow solvers; Residual schemes; Fluctuation splitting schemes; Euler equations; Unsteady flows; Unstructured meshes; Multidimensional up-winding

1. Introduction

This paper is devoted to the construction of a class of stable, accurate and *compact* methods for the solution of unsteady compressible flows on triangular unstructured meshes.

In the past decades, many numerical schemes have been devoted to the simulation of unsteady compressible flows with possibly discontinuities within the flow. In most cases, this is done with methods that are extensions of the so-called high order upwind schemes (see [20,21] for a review), even on unstructured

* Corresponding author. Tel.: +33-5-56-84-60-68; fax: +33-5-56-84-26-26.
E-mail addresses: remi.abgrall@math.u-bordeaux.fr (R. Abgrall), mezine@math.u-bordeaux.fr (M. Mezine).
[1] Also Institut Universitaire de France and Project Scalapplix, INRIA Futurs.
[2] Also Projet Scalapplix, INRIA Futurs.

0021-9991/03/$ - see front matter
doi:10.1016/S0021-9991(03)00084-6

meshes [18]. There are at least two important exceptions to this, the finite element type schemes obtained with the stream-line diffusion method [25,29], and the discontinuous Galerkin schemes [10].

The schemes constructed following the upwind high order philosophy are, for unstructured meshes, most of the time quite disappointing because they suffer from excessive numerical diffusion. To overcome this problem, one has tried to adapt ideas arising from the ENO/WENO philosophy [22,23]. Examples of such attempts are [1,19,23]. If these extensions have some success, the price to pay is very high: the coding is rather complex, and more disturbing, these schemes do not have a compact stencil, so parallel implementation becomes difficult. Lastly the analysis of the accuracy of the solution is rather unclear, or at the least difficult to carry out.

In order to tackle these two problems – compactness of the stencil, effective accuracy of the solution – at least two classes of methods have emerged in recent years, the discontinuous Galerkin schemes (DG), and the residual distribution schemes (RD) or fluctuation splitting schemes. Though different in spirit, they have a common core at least in their ''unstabilized'' versions, the residual property. This property that we discuss below in the framework of RD schemes allows us to show the formal accuracy of the scheme on a very general mesh. The DG schemes use a discontinuous polynomial representation of the unknowns which is a generalization of what is done in finite volume schemes. The solution is updated via the evaluation of fluxes, and the stabilization mechanism is obtained by very similar techniques to those in classical finite volumes. The net effect of this is to lose the residual property.

On the contrary, the RD schemes use a pointwise representation of the solution, as in finite difference schemes. The unknowns are updated by evaluation of the amount of the residual sent to the vertices, and the stabilization mechanism can be similar to artificial viscosity, as in the SUPG finite element method [26] or the stream-line diffusion method [29], or inspired by the nonlinear techniques of the so-called high resolution schemes [21,27]. One can also take into account the genuinely multidimensional structure of the problem [37].

In this paper, we consider schemes of the RD class, borrowing ideas from the upwind high order philosophy, as well as ideas coming from the stream-line diffusion one. Our goal is to propose a systematic construction of robust and high order schemes, on general meshes. This problem has received a lot of interest recently: one may quote the pioneering work of Roe and their coworkers [15,36,37], and also more recently in [2,3,14,38], but only for *steady* problems. Here we consider unsteady problems. The present paper contains, with much more details and analysis, the early draft that has been presented in the second AMIF conference, October 2000 [5]. Independently, other schemes for unsteady systems have also been recently considered [9,12,17,24] but these schemes are either a priory more computationally demanding or are not monotonicity preserving in general.

The paper is organized as follows. First, we recall some basic facts about upwind residual distribution schemes. Then we construct, for scalar problems, a class of upwind, monotonicity preserving and second order schemes. Several numerical examples are considered to show the effectiveness of our approach. Then, we extend this method, following the ideas of Abgrall and Mezine [6], first to symmetrizable systems, then to the Euler equations. The main drawback of this method is that we are constraint to a CFL like condition to preserve the monotonicity property of the scheme (not for stability purposes). Following an idea of Csik et al. [12], we then construct an unconditionally stable, monotonicity preserving, second order accurate scheme for unsteady flow problems and show several numerical examples to illustrate our technique. Some conclusions end the paper.

2. Review of residual distribution schemes

2.1. Scalar conservation law

Let us consider the two-dimensional conservation law

$$\frac{\partial u}{\partial t} + \operatorname{div} f(u) = 0 \quad \text{in } \Omega \times (0,T), \ \ \Omega \subset \mathbb{R}^2 \tag{2.1}$$

or in quasi-linear form

$$\frac{\partial u}{\partial t} + \langle \overrightarrow{\lambda}(u), \nabla u \rangle = 0, \tag{2.2}$$

where $\overrightarrow{\lambda}(u) = \partial f / \partial u$ is the advection speed. Let τ_h be a triangulation of the domain Ω. The set of triangles is $\{T_j\}_{j=1,\ldots,nt}$, the mesh points are $\{M_i\}_{i=1,\ldots,ns}$. The vertices of a triangle T are $M_{i_1}, M_{i_2}, M_{i_3}$, or i_1, i_2, i_3. When there is no ambiguity i_1, i_2, i_3 are replaced by 1, 2, 3. The discretization techniques use $\mathbb{P}_1$ finite element meshes, i.e., triangular meshes with a piecewise linear solution representation $u^h = \sum_i u_i \mathscr{N}_i$, where $\mathscr{N}_i$ is the linear shape function associated with node i. We also denote by $|T|$ the surface of the triangle T, and more generally, by $|A|$ the surface of the subset $A \subset \mathbb{R}^2$.

We define the fluctuation or the cell residual over a triangle T as the integral over this element of the spatial differential operator

$$\Phi^T = \int_T \operatorname{div} f^h \, \mathrm{d}x = |T| \, \overrightarrow{\bar{\lambda}} \cdot \nabla u^h. \tag{2.3}$$

Since ∇u^h is constant, $\overrightarrow{\bar{\lambda}}$ is a cell-averaged advection speed. If we take

$$\overrightarrow{\bar{\lambda}} = \frac{1}{|T|} \int_T \overrightarrow{\lambda}(u^h) \, \mathrm{d}x, \tag{2.4}$$

it makes an exact equivalence between the conservative form and the quasi-linear form of the cell residual, and allows us to work with the quasi-linear expression while maintaining local conservation. Expression (2.4) is called a conservative Roe-linearization. We obtain the fluctuation

$$\Phi^T = \sum_{M_i \in T} k_i u_i, \tag{2.5}$$

where $k_i = \frac{1}{2} \overrightarrow{\bar{\lambda}} \cdot n_i^T$ is called the inflow parameter, n_i^T is the scaled inward normal of the edge opposite to node i (see Fig. 1).

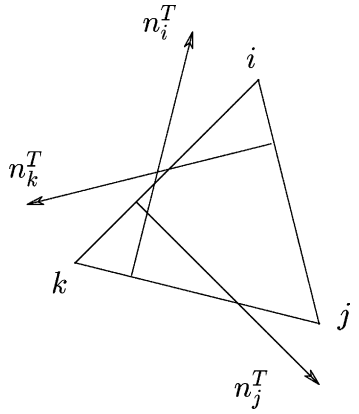

Fig. 1. Triangle with scaled inward normals.

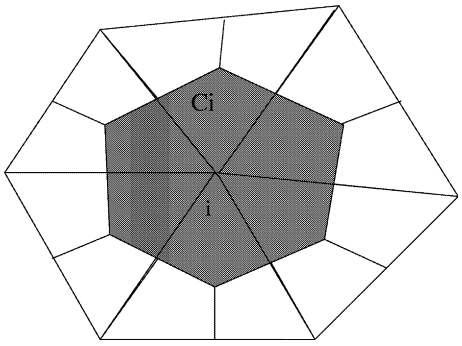

Fig. 2. The dual cell is obtained by joining the midpoints of the edges starting from M_i and the centroids of the triangles containing M_i as a vertex.

The residual distribution method consists of distributing fractions of the cell residual Φ^T to the vertices of the element. One denotes by Φ_i^T the fraction of the cell residual sent to node i. For consistency and conservation one has

$$\sum_{M_i \in T} \Phi_i^T = \Phi^T. \tag{2.6}$$

A residual distribution scheme reads

$$u_i^{n+1} = u_i^n - \frac{\Delta t}{|C_i|} \sum_{T, M_i \in T} \phi_i^T, \tag{2.7}$$

where C_i is the median dual cell around M_i (see Fig. 2).

Since u^h is continuous across edges, it can be shown [4] that, under the assumption of the standard Lax–Wendroff theorem, the limit solution is a solution of (2.1) in the linear and nonlinear case. This allows a lot of flexibility in the construction of schemes because we are not any more constrained by the geometry of the mesh. A few design principles are needed. They are: (i) upwinding, (ii) linearity preservation and (iii) monotonicity.

(i) *The upwinding property (U).* No fraction of the element residual is sent to upstream nodes

$$\Phi_i^T = 0 \quad \text{when } k_i \leqslant 0. \tag{2.8}$$

(ii) *Second order accuracy at steady state: the linear preserving condition (LP).* A way to get second order accuracy at steady state is to require that the residual Φ_i^T evaluated for the piecewise linear interpolation u^h of any smooth solution of (2.1) satisfies

$$\Phi_i^T(u^h) = \mathcal{O}(h^3), \tag{2.9}$$

see [2] for a proof. If Φ_i^T/Φ^T remains bounded when $\Phi^T \to 0$ we get second order accuracy. This follows first from the accuracy properties of the piecewise linear interpolation and second from the fact that the problem is steady. Using these two remarks, it is easy to see that the cell residual satisfies $\Phi^T = \mathcal{O}(h^3)$, so it implies (2.9).

(iii) *The monotonicity condition (P).* The scheme does not create local extrema or, if the residual sent at node i can be written as

$$\Phi_i^T = \sum_j c_{ij}(u_i - u_j), \tag{2.10}$$

we impose $c_{ij} \geqslant 0$. The scheme is L^∞ stable under a CFL condition.

2.2. Examples of schemes for scalar problems

Several schemes satisfying some or all of these design principles have been developed both in 2D and 3D. For a complete review see [33]. Some of the most popular schemes are given in Table 1: the N-scheme is a linear monotone (P) first order upwind scheme; the LDA scheme is a second order (LP) linear upwind scheme; the PSI scheme is a nonlinear second order (LP) and monotone (P) upwind scheme.

Note that a Godunov's theorem states that linear schemes (i.e., schemes for which the distribution does not depend on the solution itself) cannot be (LP) and (P) at the same time. One can get both properties only if some nonlinearity is introduced into the scheme. An example is the PSI scheme below.

One denotes $k_i^+ = \max(0, k_i)$, $k_i^- = \min(0, k_i)$.

The residual at node i for the N-scheme must satisfy the conservation relation (2.6), so we must have

$$\sum_{M_j \in T} k_j^- \widetilde{\boldsymbol{u}} = \sum_{M_j \in T} k_j^- u_j, \tag{2.11}$$

and one gets for $\widetilde{\boldsymbol{u}}$:

$$\widetilde{\boldsymbol{u}} = N \sum_{M_j \in T} k_j^- u_j \tag{2.12}$$

with

$$N = \left(\sum_{M_j \in T} k_j \right)^{-1}.$$

The PSI scheme of Struijs [37] can be obtained as a combination of the first order monotone N-scheme and the second order non-monotone LDA scheme, where $l \in \mathbb{R}$ is chosen to make the scheme monotone (P) and second order accurate at steady state (LP). It is shown in [2] that if we take $l = \max(\varphi(r_1), \varphi(r_2), \varphi(r_3))$ where

$$r_i = \frac{\Phi_i^{\mathrm{LDA}}}{\Phi_i^N}, \quad \varphi(x) = \begin{cases} x/(1-x) & \text{if } x < 0, \\ 0 & \text{else,} \end{cases} \tag{2.13}$$

the scheme satisfies the above properties.

A recent development is the proposal of modified schemes resulting from first order schemes like the N-scheme, see [6] and then [7]. The problem is formulated as follows on a general N-vertex simplex: from a low order monotone scheme $\{\Phi_i\}$, construct a high order scheme $\{\Phi_i^*\}$ such that

$$\begin{aligned} &\textstyle\sum_j \Phi_j^* = \sum_j \Phi_j = \Phi, && \text{conservation,} \\ &\Phi_j^* \Phi_j \geqslant 0, && \text{monotonicity.} \end{aligned}$$

Table 1
Residual distribution schemes

Scheme	Residual at node i	Type	U	P	LP
N	$\Phi_i^N = k_i^+(u_i - \widetilde{\boldsymbol{u}})$	Linear	$\surd$	$\surd$	
LDA	$\Phi_i^{\mathrm{LDA}} = -k_i^+ N \Phi^T$	Linear	$\surd$		$\surd$
PSI	$\Phi_i^{\mathrm{PSI}} = l\Phi_i^N + (1-l)\Phi_i^{\mathrm{LDA}}$	Nonlinear	$\surd$	$\surd$	$\surd$

We get second order accuracy under the following conditions:

$$\begin{array}{l}\Phi_j^* = \mathcal{O}(\Phi),\\ \Phi = \mathcal{O}(h^3),\end{array} \quad \text{at steady state for smooth solutions.}$$

The two conditions are important; in particular they impose second order accuracy constraints on the flux approximation $f^h(u^h)$.

Introducing

$$\beta_j = \frac{\Phi_j}{\Phi}, \quad \hat{\beta}_j = \frac{\Phi_j^*}{\Phi},$$

these conditions can be reformulated as constraints on the weights with which the residuals are distributed to the nodes

$$\begin{array}{ll}\sum_{j=1}^N \beta_j = \sum_{j=1}^N \hat{\beta}_j = 1, & \text{conservation,}\\ \beta_j\hat{\beta}_j \geqslant 0, & \text{monotonicity,}\\ \hat{\beta}_j \text{ is bounded,} & \text{high-order accuracy if } \Phi^T \text{ is small enough.}\end{array}$$

Our procedure is to impose these constraints on a mapping, which takes a set of weights $\{\beta_j\}$ corresponding to a monotone scheme (which may only be first order accurate) to a set of weights $\{\hat{\beta}_j\}$ corresponding to a scheme that is both monotone and of maximum accuracy. In reformulating, we allow for an arbitrary number N of degrees of freedom per simplex. The mapping from the N-vector $\{\beta_j\}$ to the N-vector $\{\hat{\beta}_j\}$ cannot be linear, because of the Godunov theorem, but there are many such nonlinear mappings. They are the truly multidimensional analogues of limiter functions [21] and we expect their thorough investigation to take considerable time.

Here, we simply offer two examples for the case $N = 3$, presenting the vectors $\beta = (\beta_1, \beta_2, \beta_3)$ and $\hat{\beta} = (\hat{\beta}_1, \hat{\beta}_2, \hat{\beta}_3)$ as the barycentric coordinates of a point in space with respect to an equilateral triangle. To ensure boundedness, we insist that, for all j, $0 \leqslant \hat{\beta}_j \leqslant 1$, so that the point β lies within the triangle, or on its boundary. A weaker condition, constraining the point β to a finite neighborhood of the triangle, seems possible but has not yet been explored.

If the monotone weights are all positive, then β already lies within the triangle, and it is natural to take simply $\hat{\beta} = \beta$. If β lies outside the triangle, one possibility is simply to project β onto the boundary of the triangle. For example, we may take

$$\hat{\beta}_j = \frac{\beta_j^+}{\sum_j \beta_j^+}. \tag{2.14}$$

In Fig. 3 this is shown geometrically on the left. The mapping from β to $\hat{\beta}$ is always a translation toward one of the vertices.

An alternative is to take $\hat{\beta}$ as the point on the boundary of the triangle that is closest to β. The following logic accomplishes that:

1. If β_1, β_2, β_3 are positive, define $\hat{\beta}_j = \beta_j$.
2. Else
   (a) If β_1 is negative, define $\beta_2^* = \beta_2 + \frac{1}{2}\beta_1$ and $\beta_3^* = \beta_3 + \frac{1}{2}\beta_1$.
      (i) If $\beta_2^* \leqslant 0$, $\hat{\beta}_1 = \hat{\beta}_2 = 0$, $\hat{\beta}_3 = 1$.
      (ii) If $\beta_3^* \leqslant 0$, $\hat{\beta}_1 = \hat{\beta}_3 = 0$, $\hat{\beta}_2 = 1$.
      (iii) If $\beta_2^* \geqslant 0$ and $\beta_3^* \geqslant 0$, $\hat{\beta}_1 = 0$, $\hat{\beta}_2 = \beta_2^*$ and $\hat{\beta}_3 = \beta_3^*$.
   (b) If β_2 is negative, consider (a) with the transformation of indices and change the indices according the rules $1 \to 2$, $2 \to 1$, $3 \to 3$.

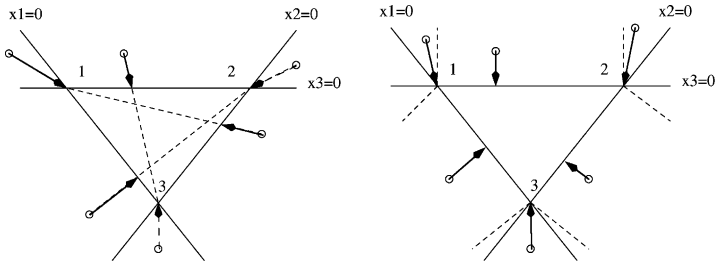

Fig. 3. Geometrical illustration of the two limiters.

(c) If β_2 is negative, consider (a) with the transformation of indices and change the indices according the rules $1 \to 3$, $2 \to 2$, $3 \to 1$

Since $\hat{\beta}_j$ is homogeneous of degree 1 in x_j, this can be coded without division. In Fig. 3 this map is shown geometrically on the right. Extension to $N \geqslant 4$ is straightforward for both maps.

2.3. Compressible Euler equations

Let us consider the compressible Euler equations in the domain $\Omega \subset \mathbb{R}^2$,

$$\frac{\partial W}{\partial t} + \operatorname{div} \mathscr{F}(W) = 0 \quad \text{in } \Omega \times (0,T), \tag{2.15}$$

or in quasi-linear form

$$\frac{\partial W}{\partial t} + A(W)\frac{\partial W}{\partial x} + B(W)\frac{\partial W}{\partial y} = 0 \quad \text{in } \Omega \times (0,T), \tag{2.16}$$

where $A(W), B(W)$ are the Jacobians of the fluxes. The flux $\mathscr{F} = (F,G)$ and the conserved variables are given by

$$\begin{aligned} &W = (\rho, \rho u, \rho v, E)^{\mathrm{T}}, \quad F(W) = (\rho u, \rho u^2 + p, \rho uv, u(E+p))^{\mathrm{T}}, \\ &G(W) = (\rho v, \rho uv, \rho v^2 + p, v(E+p))^{\mathrm{T}} \end{aligned} \tag{2.17}$$

where ρ is the density, u and v are the components of the velocity, ϵ is the internal energy, and $E = \rho\epsilon + \frac{1}{2}\rho(u^2+v^2)$ is the total energy. The equation of state is the perfect gas law

$$p = (\gamma - 1)\rho\epsilon = (\gamma - 1)\left(E - \frac{1}{2}\rho(u^2+v^2)\right),$$

where γ is the ratio of specific heats ($\gamma = 1.4$).

The construction of the residual distribution schemes is based on the quasi-linear form of the conservation law. For reasons of conservation, a particular conservative linearization is needed to generalize (2.3) and (2.4). Then the nonlinear system (2.15) is locally approximated by the linear system

$$\frac{\partial W}{\partial t} + \bar{A}\frac{\partial W}{\partial x} + \bar{B}\frac{\partial W}{\partial y} = 0, \tag{2.18}$$

where $\bar{A}$ and $\bar{B}$ are the Jacobians of the fluxes evaluated at some average state $\bar{W}$. The conservative linearization is obtained by a multidimensional extension of Roe's linearization [13,16]. Introducing Roe's

parameter vector $Z = \sqrt{\rho}(1, u, v, H)$, where H is the total enthalpy, one denotes that $W = W(Z)$ and $\mathscr{F} = \mathscr{F}(Z)$ are quadratic in Z,

$$W(Z) = \frac{1}{2}\, D(Z)Z, \quad \mathscr{F}(Z) = \frac{1}{2}\mathscr{R}(Z)Z, \tag{2.19}$$

where $D(Z)$ and $\mathscr{R}(Z)$ are matrices that depend linearly on Z. Assuming that Z has a linear variation on T, we get for the cell residual

$$\Phi^T = \sum_{M_i \in T} K_i \widetilde{W}_i, \tag{2.20}$$

where $K_i = \frac{1}{2}(\bar{A} n_i^x + \bar{B} n_i^y)$ with

$$\bar{A} = \frac{\partial F}{\partial W}(\bar{Z}), \quad \bar{B} = \frac{\partial G}{\partial W}(\bar{Z}), \quad \bar{Z} = \frac{Z_1 + Z_2 + Z_3}{3},$$

the vector $\widetilde{W}_i$ being defined as $\widetilde{W}_i = D(\bar{Z})Z_i$.

Remark 1. $(\bar{A}, \bar{B}) = \mathscr{R}(\bar{Z})D^{-1}(\bar{Z})$ are the Jacobians of the fluxes evaluated at some average state $\bar{W}$. It can be shown that the matrices K_i are diagonalizable with real eigenvalues. We set $K_i = L_i \Lambda_i R_i$ where L_i contains the left eigenvectors and R_i the right eigenvectors, and Λ_i is the diagonal matrix containing the eigenvalues.

The positive and negative parts of K_i are denoted K_i^+ and K_i^- and are defined by

$$K_i^+ = L_i \Lambda_i^+ R_i, \quad K_i^- = L_i \Lambda_i^- R_i, \tag{2.21}$$

where Λ_i^+ and Λ_i^- contains the positive and the negative eigenvalues of K_i.

The design principles for systems residual distribution schemes are similar to those defined in the previous section for scalar conservation laws, i.e.,

(i) *The upwinding property* (U). The scheme is upwind if the following condition is true: if all the eigenvalues of K_i are negative, then $\Phi_i^T = 0$.

(ii) *Second order accuracy at steady state*: *the linear preserving condition* (LP). This condition is the same as for a scalar conservation law (see [2]). A condition is to require that the residual Φ_i^T satisfies the property

$$\Phi_i^T(W^h) = \mathscr{O}(h^3) \tag{2.22}$$

for any smooth solution of (2.15), where $W^h = \frac{1}{2}D(Z^h) \cdot Z^h$ and Z^h is the piecewise linear interpolation of this solution. Note that in (2.22) what is really important is not this particular set of variables, but the fact, as shown in [2], that the interpolation of the variables or the flux is second order accurate.

(iii) *The monotonicity condition*. One wants to avoid non-physical oscillations. The formulation of this intuitive condition is difficult: however see [2] and Sections 2.4 and 4.2.4 below for details.

2.4. Examples of schemes for systems

The system N-scheme. We set

$$\Phi_i^N = \sum_j K_i^+ N K_j^- (\widetilde{W}_i - \widetilde{W}_j), \tag{2.23}$$

where $N = (\sum_j K_j^-)^{-1}$. It is shown in [2] that the matrix product $K_i^+ N$ always has a meaning, so the scheme is well defined. In [3], it is shown that for a symmetrizable system the N scheme is linearly dissipative. In the present case, if the linearization is carried out in the entropy variables $V = \nabla_W(\rho s)$, one has

$$\sum_{M_i \in T} \langle V_i, \Phi_i^N \rangle = \frac{1}{2} \sum_{M_i \in T} \langle V_i, K_i V_i \rangle + \mathscr{Q}^N(V_1, V_2, V_3) \tag{2.24}$$

with $\mathscr{Q}^N(V_1, V_2, V_3)$ a positive quadratic form.

The system LDA scheme. The system LDA scheme is defined by

$$\Phi_i^{\mathrm{LDA}} = -K_i^+ N \Phi^T. \tag{2.25}$$

Like the N-scheme, the system LDA scheme is always well defined. For symmetrizable systems no dissipation property is known.

The system N-modified scheme. The generalization of the scalar PSI scheme is not obvious. We recall the extension constructed in [2] because we use the same type of idea here.

Consider a direction $\overrightarrow{m} = (m_x, m_y)$, and the matrix $K_{\overrightarrow{m}} = m_x \bar{A} + m_y \bar{B}$. Since this matrix is diagonalizable in $\mathbb{R}$, we may consider $\ell_j,\ j = 1,4$, and $\mathbf{r}_j,\ j = 1,4$, its left and right eigenvectors. Next we consider the fluctuations $\varphi_i^j = \ell_j \cdot \Phi_i$, i.e., we decompose Φ_j onto the basis $\{\mathbf{r}_j\}$,

$$\Phi_j = \sum_{i=1}^{4} \varphi_i^j \mathbf{r}_i.$$

It is clear that

$$\ell_j \cdot \Phi = \sum_{i=1}^{3} \varphi_i^j,$$

so we may apply the procedure defined in equations (2.14), or the limiter defined by orthogonal projection. This produces a set of fluctuations $\{(\varphi_i^j)^*\}$, and we define the limited scheme by

$$\Phi_i^* = \sum_{j=1}^{4} (\varphi_i^j) \mathbf{r}_j.$$

In [6], it is shown that this scheme is LP. It is also shown that if one starts from the system N-scheme, then this scheme has a L^∞ type stability property. This property has been demonstrated on several test cases, ranging from subsonic to hypersonic cases.

In all the numerical examples presented here, we have chosen $\overrightarrow{m} = \overrightarrow{u}$. Other experiments have been done with different choices. The quality of the results is the same. The only motivation for $\overrightarrow{m} = \overrightarrow{u}$ is that this choice makes the scheme rotationally invariant, and is probably more natural.

3. Petrov–Galerkin formulation of residual distribution approach

The residual distribution schemes can be viewed as a particular class of Petrov–Galerkin finite element schemes. Denoting by w_i the Petrov–Galerkin weighting function associated to node i : $w_i = \mathscr{N}_i + \alpha_i^T$ on T, one can choose α_i^T such that the spatial discretization of the Petrov–Galerkin formulation is the same as the residual distribution approach. Starting from the finite element spatial discretization of (2.2) with constant advection speed one has

$$\sum_{T\in\tau_h}\int_T w_i\frac{\partial u^h}{\partial t}\,\mathrm{d}x+\sum_{T\in\tau_h}\int_T w_i\langle\overrightarrow{\lambda},\nabla u^h\rangle\,\mathrm{d}x=0. \tag{3.1}$$

Since $\langle\overrightarrow{\lambda},\nabla u^h\rangle$ is constant on T and equal to $\Phi^T/|T|$ one obtains

$$\sum_{T\in\tau_h}\int_T w_i\frac{\partial u^h}{\partial t}\,\mathrm{d}x+\sum_{T,M_i\in T}\int_T w_i\,\mathrm{d}x\,\frac{\Phi^T}{|T|}=0. \tag{3.2}$$

Using the definition of w_i in the second integral in equation (3.2) leads to

$$\sum_{T\in\tau_h}\int_T w_i\frac{\partial u^h}{\partial t}\,\mathrm{d}x+\sum_{T,M_i\in T}\left(\frac{1}{3}+\alpha_i^T\right)\Phi^T=0. \tag{3.3}$$

Putting $\alpha_i^T=\Phi_i^T/\Phi^T-1/3$, the spatial discretization of the Petrov–Galerkin formulation is the same as that of the residual distribution approach. The previous equation becomes

$$\sum_{T\in\tau_h}\sum_{M_j\in T}m_{ij}^T\frac{\mathrm{d}u_j}{\mathrm{d}t}+\sum_{T,M_i\in T}\Phi_i^T=0, \tag{3.4}$$

where (m_{ij}^T) is the consistent mass matrix defined by $m_{ij}^T=\int_T w_i\mathscr{N}_j\,\mathrm{d}x$. This expression is the consistent formulation of the residual distribution scheme

$$\left(m_{ij}^T\right)=\frac{|T|}{3}\begin{bmatrix}\Phi_1^T/\Phi^T+1/6 & \Phi_1^T/\Phi^T-1/12 & \Phi_1^T/\Phi^T-1/12\\ \Phi_2^T/\Phi^T-1/12 & \Phi_2^T/\Phi^T+1/6 & \Phi_2^T/\Phi^T-1/12\\ \Phi_3^T/\Phi^T-1/12 & \Phi_3^T/\Phi^T-1/12 & \Phi_3^T/\Phi^T+1/6\end{bmatrix}. \tag{3.5}$$

Remark 2. The first order N-scheme cannot be obtained from a Petrov–Galerkin approach since Φ_i^T/Φ^T are unbounded for vanishing cell residuals.

Remark 3. Starting from (3.4) we can derive a certain number of schemes, extensions of standard residual distribution schemes that have the property Φ_i^T/Φ^T bounded (see [17]).

If we want to recover (2.7) we must replace the consistent mass matrix by an inconsistent mass matrix. This matrix is obtained by lumping its element of each row to the diagonal, and replace Φ_i^T/Φ^T by 1/3 (equidistribution of the fluctuation) giving the inconsistent Galerkin lumped mass matrix (1/3)Id. This leads to the following inconsistent formulation:

$$|C_i|\frac{\mathrm{d}u_i}{\mathrm{d}t}+\sum_{T,M_i\in T}\Phi_i^T=0. \tag{3.6}$$

An explicit Euler scheme for the time derivative leads to (2.7).

For steady computations an accurate discretization of the time derivative is not required, so that (3.6) is a good alternative in place of (3.4) which requires the solution of a system of nonlinear algebraic equations. With this approximation only first order accuracy can be achieved for unsteady problems even if we use second or third accurate schemes for time derivative. So the consistent formulation (3.4) is needed to reach high order accuracy. One of the aims of this paper is to show how to construct consistent mass matrices without losing stability properties of the schemes for steady state. The development of monotone high accurate schemes using (3.4) has been considered by Ferrante [17] with a flux corrected transport formulation. He showed that positivity is lost with this formulation (the mass matrix is not guaranteed to be a

L-matrix), and to recover monotonicity he used the flux corrected transport to damp the spurious oscillations. This approach works reasonably well, but it is not a natural extension of (2.7). We lose the aspects of the residual distribution methods like: (i) upwinding, (ii) linearity preservation and (iii) compactness of the stencil (due to the FCT limiting).

The aim of this paper is to show how one can recover properties (i), (ii) and (iii).

4. Residual distribution schemes for unsteady scalar advection equations

We showed, in the previous section, that the residual distribution scheme (2.7) is not suitable for computing unsteady problems due to the inconsistent treatment of the mass matrix. Schemes with a consistent mass matrix have been considered by Caraeni, Csik et al., Ferrante, Hubbard [9,12,17,24], etc. Here we present and illustrate another solution for reaching high order accuracy for unsteady scalar advection, and in the final section, we extend it to the compressible Euler equations.

4.1. Principles

Let us consider Eq. (2.1) with constant advection speed

$$\frac{\partial u}{\partial t} + \langle \vec{\lambda}, \nabla u \rangle = 0 \text{ in } \Omega \times (0,T).$$

The idea is to see in (2.1) a steady problem in $\mathbb{R}_\xi \times \mathbb{R}_x \times \mathbb{R}_t$, where ξ is an iteration parameter. We first need to define the cell residual. For steady problems the cell residual over a triangle T is defined as the integral over this element of the operator div with the piecewise linear approximation of u on T. Here we solve the unsteady problem like a steady problem, so we define the cell residual as the integral of the differential operator $\partial_t + \text{div}$ with a space–time approximation of u on $T \times [t_n, t_{n+1}]$. To do this we need a second order approximation of u to get second order accuracy in time and space, which implies $\Phi^T = \mathcal{O}(\Delta t^3, h^3)$. The most natural choice is

$$u^h(x,t) = \frac{t - t_n}{\Delta t} u^{n+1}(x) + \frac{t_{n+1} - t}{\Delta t} u^n(x), \tag{4.1}$$

where u^n and u^{n+1} are respectively the piecewise linear approximation of u at time t_n and t_{n+1}. Hence we define the residual Φ^T by

$$\Phi^T = \int_{t_n}^{t_{n+1}} \int_T \frac{\partial u^h}{\partial t} + \langle \lambda, \nabla u^h \rangle \, \mathrm{d}x \, \mathrm{d}t. \tag{4.2}$$

After calculations, we get

$$\Phi^T = \frac{|T|}{3} \sum_{M_i \in T} \left(u_i^{n+1} - u_i^n \right) + \frac{\Delta t}{2} \sum_{M_i \in T} k_i \left(u_i^{n+1} + u_i^n \right), \tag{4.3}$$

with the same definition of k_i. We denote by $\Phi_{i,n}$ and $\Phi_{i,n+1}$ the residuals sent to the nodes (M_i, t_n) and (M_i, t_{n+1}).

The residual (4.2) is the fluctuation computed over the prism $K = T \times [t_n, t_{n+1}]$ (see Fig. 4). Our approach is a space–time interpretation of the classical residual distribution methods with the linear in time and in space approximation of the solution (4.1). We need to distribute this fluctuation to the vertices of the prism K: upwinding in time, i.e., a causality principle, leads us to distribute the time–space residual to the nodes located at time t_{n+1}, so one has $\Phi_{i,n} = 0$.

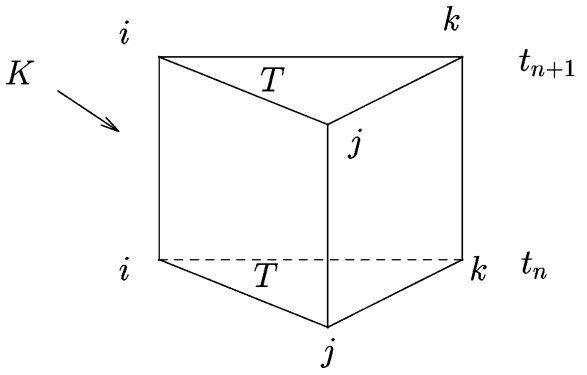

Fig. 4. The prism K defined by the triangle T.

The residual distribution scheme reads

$$\forall M_i \in \tau_h, \quad \sum_{T, M_i \in T} \Phi_{i,n+1} = 0, \tag{4.4}$$

where $\Phi_{i,n+1}$ is the residual sent to node M_i at time t_{n+1}. From now on we replace $\Phi_{i,n+1}$ by Φ_i since there is no possible confusion. The residuals are assumed to fulfill the conservation relation

$$\sum_{M_i \in T} \Phi_i = \Phi, \tag{4.5}$$

where Φ is given by (4.3).

4.1.1. Design principles

(i) *The upwinding property*. No fraction of the element residual is sent to nodes for time $t = t_n$. Eq. (4.4) means that all the residual of K is sent to time t_{n+1}.

(ii) *The linear preserving condition (LP)*. The LP property is the same as for the steady case: if the solution is smooth then

$$\Phi_i = \mathcal{O}(h^3, \Delta t^3).$$

(iii) *No spurious oscillations in the solution.*

4.2. Extension of classical schemes

We discuss a space–time N-scheme and LDA scheme that reduces to the classical N-scheme and LDA scheme for steady state applications. This space–time schemes allow us to construct space–time blending and modified schemes.

4.2.1. The N-scheme

We set

$$\Phi_i^N = \frac{|T|}{3}\left(u_i^{n+1} - u_i^n\right) + \frac{\Delta t}{2} k_i^+ \left(u_i^{n+1} - \widetilde{u}^{n+1}\right) + \frac{\Delta t}{2} k_i^+ \left(u_i^n - \widetilde{u}^n\right),$$

where $\widetilde{u}^n$ and $\widetilde{u}^{n+1}$ are computed to have the conservation relation (4.5). One gets

$$\widetilde{u}^n = N\sum_{M_j\in T} k_j^- u_j^n, \quad \widetilde{u}^{n+1} = N\sum_{M_j\in T} k_j^- u_j^{n+1}$$

with the same definition of N (see Section 2.4). The residual at node i becomes

$$\Phi_i^N = \frac{|T|}{3}\left(u_i^{n+1}-u_i^n\right) + \frac{\Delta t}{2}\sum_{M_j\in T}\left[k_i^+ N k_j^-\left(u_i^{n+1}-u_j^{n+1}\right) + k_i^+ N k_j^-\left(u_i^n - u_j^n\right)\right]. \tag{4.6}$$

The schemes reads, for all $M_i \in \tau_h$,

$$\sum_{T,M_i\in T}\left[\frac{|T|}{3}\left(u_i^{n+1}-u_i^n\right) + \frac{\Delta t}{2}\sum_{M_j\in T}\left[k_i^+ N k_j^-\left(u_i^{n+1}-u_j^{n+1}\right) + k_i^+ N k_j^-\left(u_i^n - u_j^n\right)\right]\right] = 0. \tag{4.7}$$

Remark 4.

1. For steady computations, we recover the standard N-scheme.
2. One of the reasons for splitting space and time like equation (4.6) is that the conservation relation is met and positivity can be shown, see below. Another constraint comes from the fact the scheme (4.7) is implicit in time: the linear system has to be solvable. This last point was a motivation for the present splitting: we also tried many combinations, but none were leading to solvable systems except the choice (4.6).

The scheme (4.7) is an implicit scheme, which can be written as $AU^{n+1} = BU^n$ where U^{n+1} and U^n are respectively the vectors of unknowns at time t_{n+1} and t_n. The entries of the matrices A and B are given by

$$A_{ii} = \sum_{T,M_i\in T}\left(\frac{|T|}{3} + \frac{\Delta t}{2}k_i^+\right), \quad A_{ij} = \sum_{T,(M_i,M_j)\in T} -\frac{\Delta t}{2}k_i^+ N k_j^-, \tag{4.8}$$

$$B_{ii} = \sum_{T,M_i\in T}\left(\frac{|T|}{3} - \frac{\Delta t}{2}k_i^+\right), \quad B_{ij} = \sum_{T,(M_i,M_j)\in T} \frac{\Delta t}{2}k_i^+ N k_j^-, \tag{4.9}$$

and we have the following lemma:

Lemma 1. *The matrix A is non-singular and is a L-matrix, i.e., $A_{ii} > 0\ \forall i$ and $A_{ij} \leqslant 0$ for $j \neq i$.*

Proof. One has $A_{ii} > 0$ and $A_{ij} \leqslant 0$ since $N < 0 \Rightarrow k_i^+ N k_j^- \geqslant 0$, hence A is a L-matrix.

To prove that A is non-singular we show that A is a diagonally strictly dominant matrix, i.e.,

$$\forall i \quad |A_{ii}| > \sum_{j\neq i}|A_{ij}|.$$

We have

$$\begin{aligned}
|A_{ii}| - \sum_{M_j\neq M_i}|A_{ij}| &= \sum_{T,M_i\in T}\left(\frac{|T|}{3} + \frac{\Delta t}{2}k_i^+\right) - \sum_{M_j\neq M_i}\sum_{T,(M_i,M_j)\in T}\frac{\Delta t}{2}k_i^+ N k_j^- \\
&= \sum_{T,M_i\in T}\left(\frac{|T|}{3} + \frac{\Delta t}{2}k_i^+\right) - \sum_{T,M_i\in T}\sum_{M_j\neq M_i}\frac{\Delta t}{2}k_i^+ N k_j^- = \sum_{T,M_i\in T}\left(\frac{|T|}{3} + \frac{\Delta t}{2}k_i^+\right) - \sum_{T,M_i\in T}\frac{\Delta t}{2}k_i^+ \\
&= \sum_{T,M_i\in T}\frac{|T|}{3} = |C_i| > 0.
\end{aligned}$$

This shows that A is diagonally strictly dominant. This achieves the proof. □

We remark that $B_{ij} \geqslant 0$ for $j \neq i$, and under the condition $\Delta t \leqslant \frac{2}{3}(|T|/k_i^+)$ one has $B_{ii} \geqslant 0$. The monotonicity property of the scheme is described in the following:

Proposition 4.1. The extension of the N-scheme defined by (4.7) is monotone under the CFL like condition

$$\Delta t \leqslant \frac{2}{3} \min_{T, M_i \in T} \frac{|T|}{k_i^+}. \tag{4.10}$$

Remark 5.

(1) This result states that the scheme is monotonicity preserving, at least under a CFL like condition. This is a statement of stability in the L^∞ norm. This is not a statement on the L^2 stability, in other words, we are not saying that this implicit scheme is only stable under condition (4.10). To anticipate a bit the results of this paper, we show in Appendix A in a more complex case for which the scalar one is a very particular example, that this scheme is *unconditionally* stable in L^2.

(2) Condition (4.10) seems to be a severe limit on the allowed time step but computations with CFL great than one have shown that monotonicity is preserved. A close look at the proof indicates that this condition is certainly not optimal. In Section 6, using an idea of Csik et al. [12], we show how to avoid this severe constraint.

Proof. The scheme can be written as $AU^{n+1} = BU^n$ with A a non-singular L-matrix, and B a matrix with positive elements. It is shown in [30] that if A is a regular L-matrix the following assertions are equivalent:

(i) A^{-1} is positive,

(ii) there exists a diagonal positive matrix D such that $D^{-1}AD$ is diagonally strictly dominant.

We apply this results with $D = Id$ so it implies that A^{-1} is positive. B has positive elements, thus the matrix $A^{-1}B$ is positive.

Step 1: Suppose there exists $a \in \mathbb{R}$ such that $u_i^n \geqslant a$ for all $M_i \in \tau_h$. One wants to show $u_i^{n+1} \geqslant a$ for all $M_i \in \tau_h$.

One has

$$\sum_{M_i \in T} \left(\frac{|T|}{3}\left(u_i^{n+1} - u_i^n\right) + \frac{\Delta t}{2} \sum_{M_j \neq M_i} k_i^+ N k_j^- \left(u_i^{n+1} - u_j^{n+1} + u_i^n - u_j^n\right) \right) = 0,$$

$$\begin{aligned}
&\sum_{M_i \in T} \left(\frac{|T|}{3} u_i^{n+1} + \frac{\Delta t}{2} \sum_{M_j \neq M_i} k_i^+ N k_j^- \left(u_i^{n+1} - u_j^{n+1}\right) \right) = \sum_{M_i \in T} \left(\frac{|T|}{3} u_i^n - \frac{\Delta t}{2} \sum_{M_j \neq M_i} k_i^+ N k_j^- \left(u_i^n - u_j^n\right) \right) \\
&= \sum_{M_i \in T} \left(\left(\frac{|T|}{3} - \frac{\Delta t}{2} k_i^+ \right) u_i^n + \frac{\Delta t}{2} \sum_{M_j \neq M_i} k_i^+ N k_j^- u_j^n \right) \geqslant \sum_{M_i \in T} \left(\left(\frac{|T|}{3} - \frac{\Delta t}{2} k_i^+ \right) a \right. \\
&\left. + \frac{\Delta t}{2} \sum_{M_j \neq M_i} k_i^+ N k_j^- a \right) \geqslant \sum_{M_i \in T} \frac{|T|}{3} a,
\end{aligned} \tag{4.11}$$

because the matrix B is positive. The inequalities (4.11) imply that

$$\sum_{M_i \in T} \left(\frac{|T|}{3}\left(u_i^{n+1} - a\right) + \frac{\Delta t}{2} \sum_{j \neq i} k_i^+ N k_j^- \left(\left(u_i^{n+1} - a\right) - \left(u_j^{n+1} - a\right)\right) \right) \geqslant 0,$$

which can be rewritten as

$$A(u^{n+1} - a) \geqslant 0.$$

The matrix A^{-1} is positive so one has $u^{n+1} - a \geqslant 0$, i.e., $u_i^{n+1} \geqslant a$ for all $M_i \in \tau_h$.

Step 2: Suppose that there exists $a \in \mathbb{R}$ such that $u_i^n \leqslant a$ for all $M_i \in \tau_h$. One wants to show $u_i^{n+1} \leqslant a$ for all $M_i \in \tau_h$. We do the same thing as before. This achieves the proof. □

4.2.2. The LDA scheme

This scheme directly follows from the consistent formulation (3.4) with Crank–Nicholson discretization for the time derivative, using the standard LDA scheme. Consider expression (3.4) with the standard LDA scheme

$$\sum_{T,M_i\in T}\sum_{M_j\in T} m_{ij}^T \frac{\mathrm{d}u_j}{\mathrm{d}t} + \sum_{T,M_i\in T}\left(-k_i^+ N\right)\Phi^T(u^h) = 0,$$

where $u^h = \sum_j u_j(t)\mathcal{N}_j$. If we consider Crank–Nicholson discretization of time derivative one obtains

$$\begin{aligned}
&\sum_{T,M_i\in T}\sum_{M_j\in T} m_{ij}^T\left(u_j^{n+1} - u_j^n\right) + \frac{1}{2}\sum_{T,M_i\in T}\left(-k_i^+ N\right)\left(\Phi^T(u^{n+1}) + \Phi^T(u^n)\right) = 0,\\
&\sum_{T,M_i\in T}\sum_{M_j\in T} m_{ij}^T\left(u_j^{n+1} - u_j^n\right) + \frac{1}{2}\sum_{T,M_i\in T}\left(-k_i^+ N\right)\left(\sum_j k_j\left(u_j^{n+1} + u_j^n\right)\right) = 0,
\end{aligned} \tag{4.12}$$

After lengthy calculations, expression (4.12) can be written as

$$\sum_{T,M_i\in T}\Phi_i^{\mathrm{LDA}} = 0$$

with Φ_i^{LDA} defined by

$$\begin{aligned}
\Phi_i^{\mathrm{LDA}} = {}& \frac{|T|}{3}\left(-k_i^+ N + \frac{1}{6}\right)\left(u_i^{n+1} - u_i^n\right) + \frac{|T|}{3}\left(-k_i^+ N - \frac{1}{12}\right)\sum_{M_j\neq M_i}\left(u_j^{n+1} - u_j^n\right)\\
&- \frac{\Delta t}{2}k_i^+ N\sum_{M_j\in T} k_j\left(u_j^{n+1} + u_j^n\right).
\end{aligned} \tag{4.13}$$

As for the extension of the N-scheme, we write the LDA scheme as $AU^{n+1} = BU^n$. The matrices A and B have no apparent properties.

Remark 6. We recover the LDA scheme of Ferrante [17].

4.2.3. The PSI scheme

The extension of the PSI scheme is straightforward. It is a result of a combination of the first order monotone N-scheme (4.7) and the second order non-monotone LDA scheme (4.13)

$$\Phi_i^{\mathrm{PSI}} = l\Phi_i^N + (1-l)\Phi_i^{\mathrm{LDA}}, \tag{4.14}$$

where $l = \max(\varphi(r_1), \varphi(r_2), \varphi(r_3))$ with

$$r_i = \frac{\Phi_i^{\mathrm{LDA}}}{\Phi_i^N}, \quad \varphi(x) = \begin{cases} x/(1-x) & \text{if } x < 0,\\ 0 & \text{else.}\end{cases}$$

We have experimentally noticed that the blending parameter, proposed for steady state by Deconinck and van der Weide, defined by

$$l = \frac{|\Phi^T|}{\sum_{M_j \in T} |\Phi_j^N|} \tag{4.15}$$

works very well, even though it does not satisfy the positivity requirements (we have found numerical counter-examples).

In fact, the only case we are aware of such a scheme which is proved to be positive is for steady problems where one can recover the PSI scheme of Struijs. In the case of unsteady problems, the use of a genuine multidimensional space time scheme such as the one introduced by Csik et al. [12] would certainly not produce a *provable* positive scheme, even though they show it works very well on many cases. The reason is that there might be three target configurations (the space–time element is a prism), and we only have one free parameter (the blending parameter). Positivity is translated into three inequalities as in [2], so too many constraints to satisfy. The only case in which one parameter would probably be enough is when the faces of the time–space element introduced in [12] are characteristic. This is exceptional.

We need to solve a system of nonlinear equations. This is done by Newton's method. One can write the PSI scheme as $F(U^{n+1}) = 0$,

$$\begin{aligned} F: \quad & \mathbb{R}^{ns} \to \mathbb{R}^{ns} \\ & U \mapsto (F_i(U))_{i=1,\ldots,ns}, \end{aligned}$$

where $F_i(U) = \sum_{T, M_i \in T} \Phi_i^{\mathrm{PSI}}$. The kth step of Newton's method is

$$U^{k+1} = U^k - \widetilde{J}(U^k) F(U^k),$$

where $\widetilde{J}(U^k) = \partial F / \partial U$ evaluated at point U^k.

4.2.4. The N-modified scheme

The N-modified scheme is described in [6]. We set

$$\phi_i^{NM} = \Phi_i^N + \Psi_i, \tag{4.16}$$

Ψ_i is computed to get second order accuracy and positivity *exactly* as for the modified scheme of Section 2.2 where the space residuals are replaced by the space–time residuals (4.6). The difference is that the evaluation of the limiter is implicit: since the sum of the Φ_i^Ns is the space–time residual Φ over the prism $T \times [t_n, t_{n+1}]$ and since the terms Ψ_i are computed so that ϕ_i^{NM} is proportional to Φ while we keep the monotonicity property, the two time layers t_n and t_{n+1} are necessarily coupled. The nonlinear equations are solved as in the previous section, using a Newton algorithm.

4.3. Numerical results

4.3.1. The rotating cosine hill

The rotating cosine hill is a classical test case for numerical schemes of the two-dimensional linear unsteady advection equation. The test consists in the transport of a cosine shape by a circular advection field centered at the origin

$$\frac{\partial u}{\partial t} + \langle \overrightarrow{\lambda}, \nabla u \rangle = 0 \quad \text{in } [-1,1] \times [-1,1], \tag{4.17}$$

where $\lambda = (y, -x)^T$. The initial solution is $(1 + \cos(4\pi\sqrt{(x+0.5)^2 + y^2}))/2$ if $r = \sqrt{(x+0.5)^2 + y^2} \leqslant \frac{1}{8}$ and 0 elsewhere. The solution is set to zero at the inflow boundaries, at each time step.

The computation was made on an unstructured grid of 8079 nodes and 15836 elements. The time step was taken to satisfy condition (4.10):

$$\Delta t = \frac{2}{3}\mathrm{CFL}\min_i \frac{|T|}{k_i^+} \tag{4.18}$$

with $\mathrm{CFL} = 0.9$. The results, using the schemes described in the previous section and the MUSCL scheme (with *minmod* limiter and Runge–Kutta integration in time) after one revolution are compared in Fig. 5. We provide the cross-section at $y = 0$ in Fig. 7. The N-scheme is clearly the most diffusive (see also Table 2), streamwise and crosswise diffusion being considerable. The LDA scheme keeps the height of the peak much better but the monotonicity is not preserved. The PSI and N-modified schemes give similar results but the N-modified scheme is the less diffusive with a peak value of 0.802. This results are much better than those obtained by the MUSCL scheme.

4.3.2. The rotating cylinder

This test case differs from the previous only for the initial profile

$$u(x,y) = \begin{cases} 1 & \text{for } r < 0.25, \\ 0 & \text{else}, \end{cases} \tag{4.19}$$

where $r = \sqrt{(x+0.5)^2 + y^2}$, which is not continuous, contrary to the previous case. The computation was made on the same grid with a CFL of 0.9, the results after one revolution being displayed in Fig. 6. The solutions exhibit the same properties as the rotating cosine hill. Cross-sections of the solutions after one revolution are provided in Fig. 8. The PSI scheme and N-modified scheme give similar results. These results are better than MUSCL scheme. The LDA scheme exhibits spurious oscillations, as expected.

In both cases, the limited N-scheme and the blended-PSI behave the same. However, the modified N-scheme CPU cost is about half that of the blended scheme, because one has no need to evaluate the LDA scheme.

4.4. Conclusions for the scalar problems

We have considered two different techniques for increasing the accuracy of unsteady problems, the PSI-blending and the N-modified schemes. The results are roughly speaking similar, with a slight advantage for the N-modified scheme, in terms of accuracy and efficiency. It is possible to extend the PSI-blending technique to systems, following [2]. This has been done elsewhere and we do not report our results here. This technique works quite well but in some cases, for example the interaction of a vortex and a shock (see Section 5.3.4) or the ramp problem (see Section 5.3.3), the results are disappointing: there are some slight oscillations across the shocks.

For these reasons we have abandoned this technique, and we do not consider it anymore.

5. Residual distribution schemes for the unsteady Euler equations

Consider the system of Euler equations

$$\frac{\partial W}{\partial t} + \mathrm{div}\mathscr{F}(W) = 0,$$

where W and $\mathscr{F}$ are given by (2.17). The system is closed by the perfect gas law.

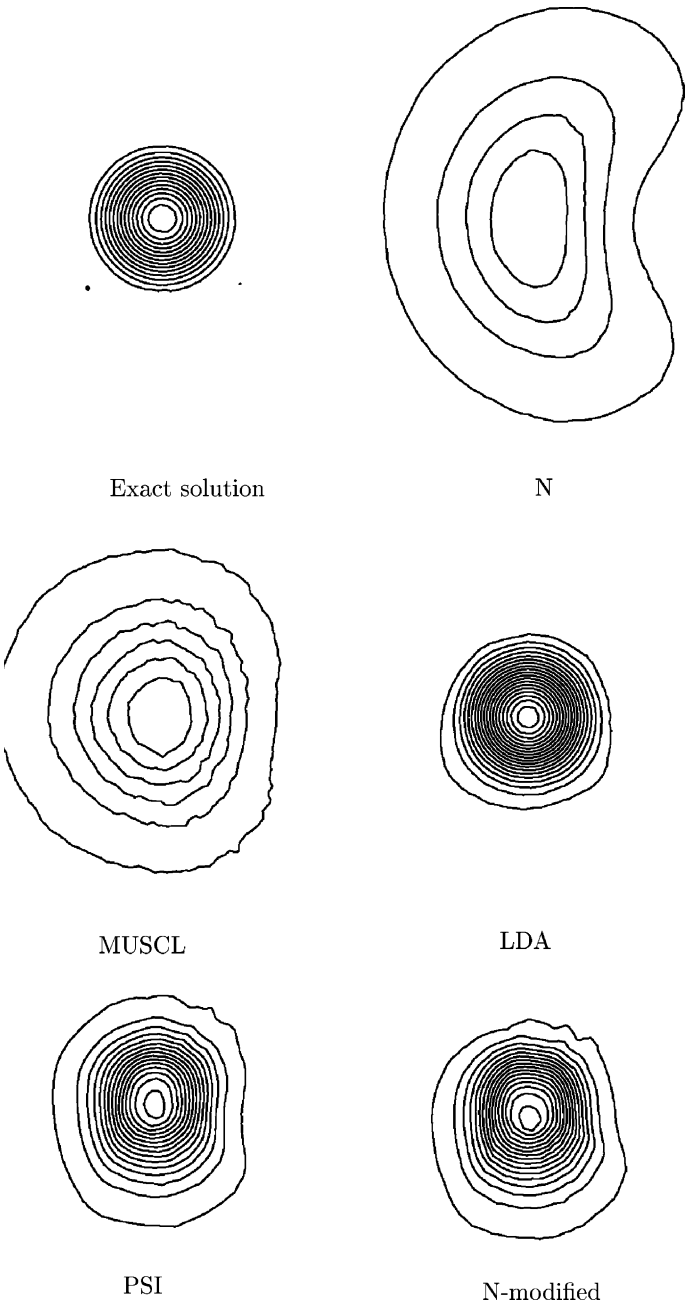

Fig. 5. Solutions for the rotating cosine hill after one revolution.

The construction of the residual distribution schemes, described in the previous section, is based on the quasi-linear form of the convection equations (as for steady schemes) and a space–time approximation of the unknowns. So extension to the unsteady Euler equations needs to use: (i) a second order approximation of W and $\mathscr{F}$ in order to get second order accuracy; (ii) a conservative linearization.

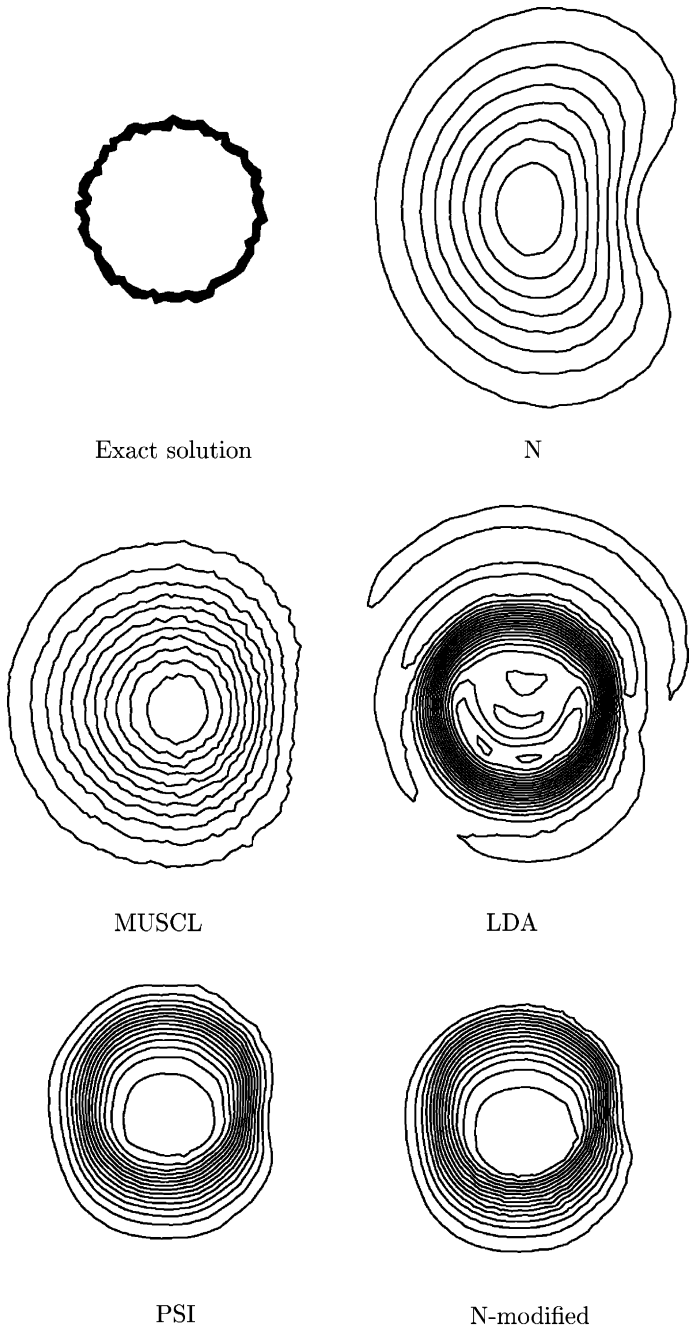

Fig. 6. Solutions for the rotating cylinder after one revolution.

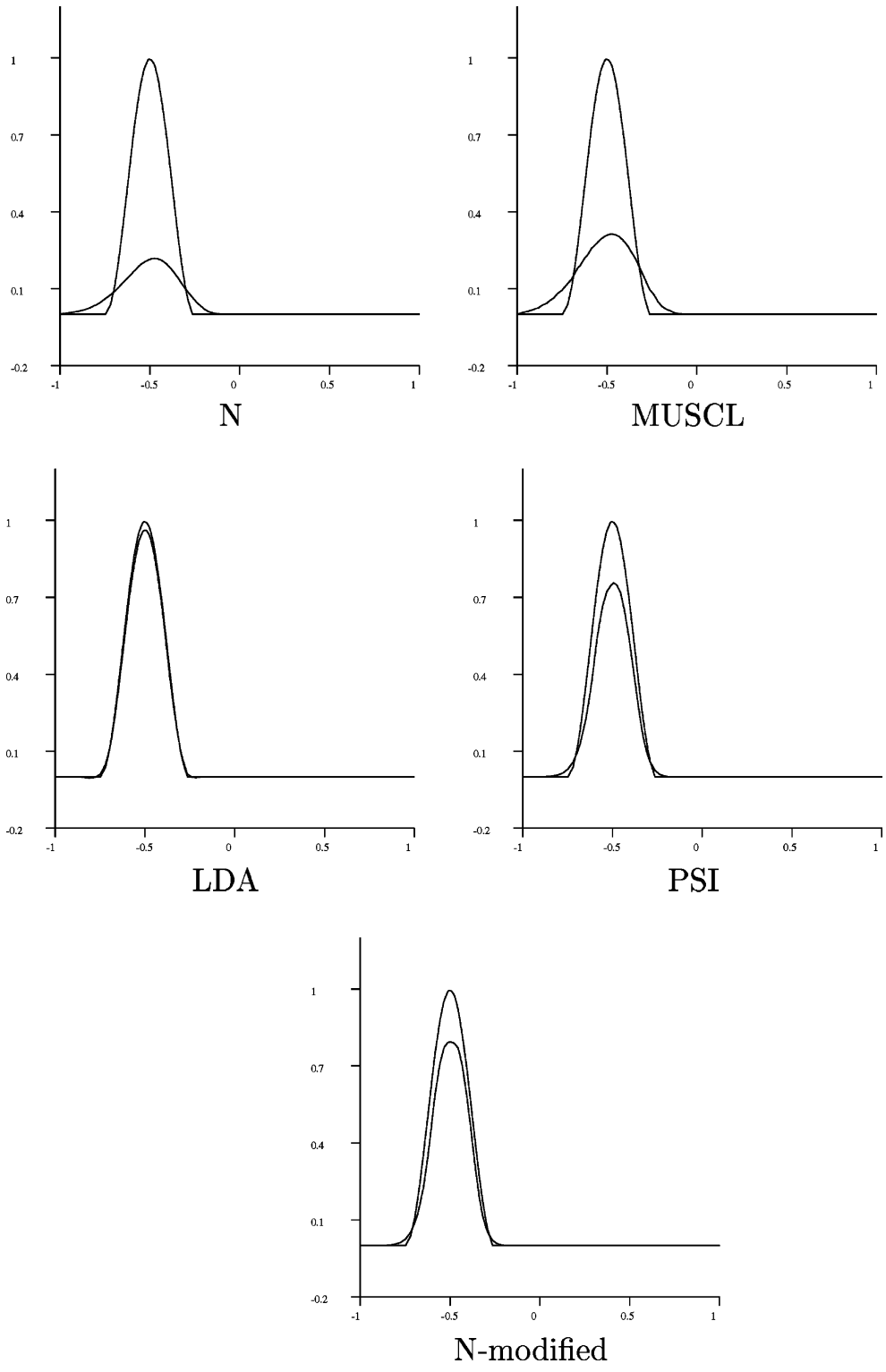

Fig. 7. Sections at $y = 0$ of the solutions for the rotating cosine.

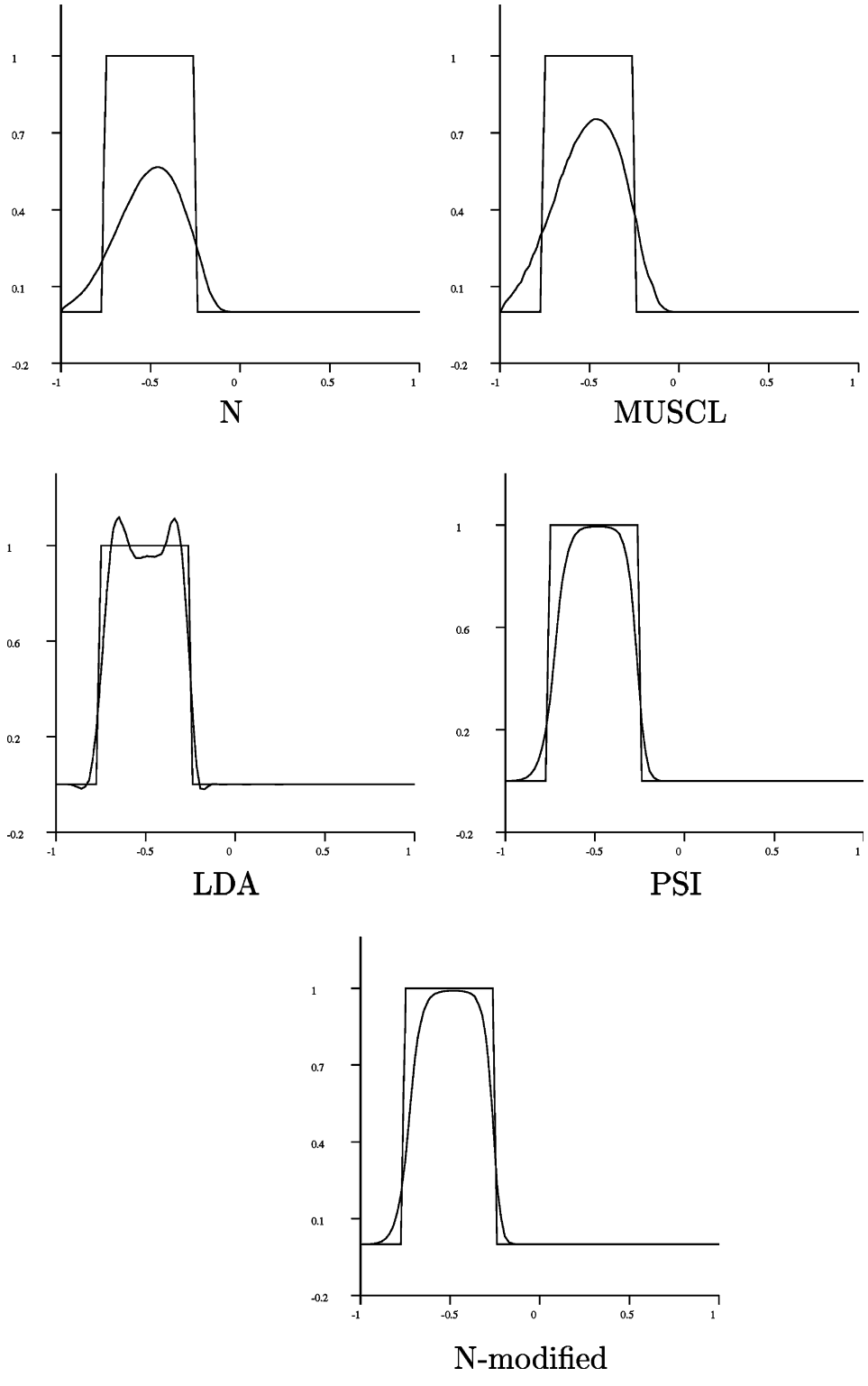

Fig. 8. Sections at $y = 0$ of the solutions for the rotating cylinder.

Table 2
Min and Max solution values for the rotating cosine hill test case

Scheme	Min	Max
N	0	0.217
MUSCL	0	0.313
LDA	−0.03	0.983
PSI	0	0.756
N-modified	0	0.802

5.1. The cell residual

The cell residual over a triangle T is given by

$$\Phi^T = \int_{t_n}^{t_{n+1}} \int_T \left(\frac{\partial W^h}{\partial t} + \operatorname{div} \mathscr{F}^h \right) \mathrm{d}x\,\mathrm{d}t,$$

where W^h and $\mathscr{F}^h$ are respectively the space–time approximation of the solution and the fluxes. This approximation is obtained using Roe's parameter vector Z. We set

$$W^h = \frac{t - t_n}{\Delta t} W^{n+1} + \frac{t_{n+1} - t}{\Delta t} W^n,$$

$$\mathscr{F}^h = \frac{t - t_n}{\Delta t} \mathscr{F}^{n+1} + \frac{t_{n+1} - t}{\Delta t} \mathscr{F}^n,$$

where $W^s = W(Z^s)$ and $\mathscr{F}^s = \mathscr{F}(Z^s)$ and Z^s being the piecewise linear approximation of Z at time s (t_n or t_{n+1}). One has

$$\Phi^T = I_1 + I_2 \qquad \text{with } I_1 = \int_{t_n}^{t_{n+1}} \int_T \frac{\partial W^h}{\partial t} \mathrm{d}x\,\mathrm{d}t, \quad I_2 = \int_{t_n}^{t_{n+1}} \int_T \operatorname{div} \mathscr{F}^h \mathrm{d}x\,\mathrm{d}t.$$

For I_1 we have

$$I_1 = \int_{t_n}^{t_{n+1}} \frac{\partial W}{\partial t} \mathrm{d}x\,\mathrm{d}t = \int_T \frac{D(Z^{n+1})Z^{n+1} - D(Z^n)Z^n}{2} \mathrm{d}x.$$

Moreover,

$$\begin{aligned} \int_T D(Z)Z\,\mathrm{d}x &= \frac{|T|}{3} \left(D\left(\frac{Z_1 + Z_2}{2}\right) \frac{Z_1 + Z_2}{2} + D\left(\frac{Z_1 + Z_3}{2}\right) \frac{Z_1 + Z_3}{2} + D\left(\frac{Z_2 + Z_3}{2}\right) \frac{Z_2 + Z_3}{2} \right) \\ &= \frac{|T|}{12} \sum_{M_i \in T} D(Z_i)Z_i + \frac{|T|}{4} \sum_{M_i \in T} D(\overline{Z})Z_i = \frac{|T|}{6} \sum_{M_i \in T} W_i + \frac{|T|}{4} \sum_{M_i \in T} \widetilde{W}_i, \end{aligned}$$

because $D(Z)Z$ is quadratic in Z. I_1 becomes

$$I_1 = \frac{|T|}{4} \sum_{M_j \in T} \left[\left(\frac{1}{3} W_j^{n+1} + \frac{1}{2} \widetilde{W}_j^{n+1} \right) - \left(\frac{1}{3} W_j^n + \frac{1}{2} \widetilde{W}_j^n \right) \right].$$

Now we compute I_2,

$$I_2 = \int_{t_n}^{t_{n+1}} \int_T \operatorname{div} \mathscr{F} \, \mathrm{d}x \, \mathrm{d}t = \frac{\Delta t}{2} \int_T \operatorname{div} \mathscr{F}^{n+1} + \operatorname{div} \mathscr{F}^n \, \mathrm{d}x$$
$$= \frac{\Delta t}{2} \int_T \mathscr{R}(Z^{n+1}) \, \mathrm{d}x \cdot \nabla Z^{n+1} + \frac{\Delta t}{2} \int_T \mathscr{R}(Z^n) \, \mathrm{d}x \cdot \nabla Z^n = \frac{\Delta t}{2} \sum_{M_j \in T} \frac{\mathscr{R}(\bar{Z}^{n+1}) \cdot n_j^T}{2} Z_j^{n+1} + \frac{\mathscr{R}(\bar{Z}^n) \cdot n_j^T}{2} Z_j^n.$$

Setting

$$K_j^{n+1} = \frac{1}{2} \left\langle \mathscr{R}(\bar{Z}^{n+1}) D^{-1}(\bar{Z}^{n+1}), n_j^T \right\rangle$$

and

$$K_j^n = \frac{1}{2} \left\langle \mathscr{R}(\bar{Z}^n) D^{-1}(\bar{Z}^n), n_j^T \right\rangle,$$

the cell residual is given by

$$\Phi^T = \frac{|T|}{4} \sum_{M_j \in T} \left[\left(\frac{1}{3} W_j^{n+1} + \frac{1}{2} \widetilde{W}_j^{n+1} \right) - \left(\frac{1}{3} W_j^n + \frac{1}{2} \widetilde{W}_j^n \right) \right] + \frac{\Delta t}{2} \sum_{M_j \in T} K_j^{n+1} \widetilde{W}_j^{n+1} + K_j^n \widetilde{W}_j^n, \tag{5.1}$$

where $\widetilde{W}_j^n = D(\bar{Z}^n) Z_j^n$ and $\widetilde{W}_j^{n+1} = D(\bar{Z}^{n+1}) Z_j^{n+1}$.

This expression is similar to (4.3), but a difficulty appears with the presence of terms K_j^{n+1} which are computed at time t_{n+1} (due to the nonlinearity of the Euler equations). Therefore system residual distribution schemes for unsteady computations are intrinsically implicit in time. This is solved thanks to a Newton method.

5.2. System residual distribution schemes

In this section we give the generalization of the unsteady scalar schemes described in Section 4.2.

5.2.1. The system N-scheme

For a scalar advection equation one has

$$\phi_i^N = \frac{|T|}{3} \left(u_i^{n+1} - u_i^n \right) + \frac{\Delta t}{2} k_i^+ \left(u_i^{n+1} - \widetilde{u}^{n+1} \right) + \frac{\Delta t}{2} k_i^+ \left(u_i^n - \widetilde{u}^n \right), \tag{5.2}$$

where $\widetilde{u}^n$ and $\widetilde{u}^{n+1}$ are computed to have the conservation relation (4.5). We set

$$\phi_i^N = \frac{|T|}{4} \left[\left(\frac{1}{3} W_i^{n+1} + \frac{1}{2} \widetilde{W}_i^{n+1} \right) - \left(\frac{1}{3} W_i^n + \frac{1}{2} \widetilde{W}_i^n \right) \right] + \frac{\Delta t}{2} K_i^{n+1^+} \left(\widetilde{W}_i^{n+1} - W_{n+1}^* \right) + \frac{\Delta t}{2} K_i^{n^+} \left(\widetilde{W}_i^n - W_n^* \right). \tag{5.3}$$

If $\widetilde{W}^{n+1}$ and $\widetilde{W}^n$ are computed to make the scheme conservative, one gets

$$W_{n+1}^* = N^{n+1} \sum_{M_j \in T} K_j^{n+1^-} \widetilde{W}_j^{n+1}, \quad W_n^* = N^n \sum_{M_j \in T} K_j^{n^-} \widetilde{W}_j^n \tag{5.4}$$

with $N^n = \left(\sum_{M_j \in T} K_j^{n^-} \right)^{-1}$ and $N^{n+1} = \left(\sum_{M_j \in T} K_j^{n+1^-} \right)^{-1}$.

Remark 7. The matrices $N^n K_j^n$ and $N^{n+1} K_j^{n+1}$ always exist (see [2]), so the system N-scheme is well defined.

In Appendix A, we show that this system is unconditionally energy stable.

5.2.2. The system LDA scheme

We set

$$\Phi_i^{\mathrm{LDA}} = \left(-\left(K_i^+ N\right)^{n+1} + \frac{1}{6}\mathrm{Id}\right)\Phi_i^T + \left(-\left(K_i^+ N\right)^{n+1} - \frac{1}{12}\mathrm{Id}\right)\sum_{M_j \neq M_i} \Phi_j^T - \left(K_i^+ N\right)^{n+1}\Phi^s,$$

where

$$\Phi_j^T = \frac{|T|}{4}\left[\left(\frac{1}{3}W_j^{n+1} + \frac{1}{2}\widetilde{W}_j^{n+1}\right) - \left(\frac{1}{3}W_j^n + \frac{1}{2}\widetilde{W}_j^n\right)\right]$$

and

$$\Phi^s = \frac{\Delta t}{2}\sum_{j\in T} K_j^{n+1}\,\widetilde{W}_j^{n+1} + K_j^n\,\widetilde{W}_j^n.$$

Remark 7 also applies to the LDA scheme.

5.2.3. The system N-modified scheme

The idea is similar to than the one developed in [6]. We present here a summary of these results, and we refer to the above reference for a detailed presentation.

For the sake of simplicity, let us explain our procedure on the linearized $d \times d$ system

$$\frac{\partial W}{\partial t} + A\frac{\partial W}{\partial x} + B\frac{\partial W}{\partial y} = 0,$$

where we assume A and B symmetric.

Since for any (α, β) the matrix $\alpha A + \beta B$ is symmetric, there exists a complete set of eigenvectors $\{r_j\}_{j=1,d}$.

Following [6], we introduce the simple waves

$$U_\sigma(x,t) = (t - t_0)(\alpha x + \beta y)r_\sigma,$$

where r_σ is any eigenvector in $\{r_j\}_{j=1,d}$ and λ_σ is the associated eigenvalue. We first notice that any function

$$W(x,t) = \frac{t - t_n}{\Delta t}W^{n+1}(x) + \frac{t_{n+1} - t}{\Delta t}W(x),$$

where W^n and W^{n+1} are linear in x, is a sum of $3 \times d \times 2$ simple waves plus possibly a constant. This number of waves comes from the fact that a triangle has three vertices, so there are three basis functions, any vector $W \times \mathcal{N}_j(x)$ can be decomposed into the sum of d orthogonal vectors, and we have to do so at times t_n and t_{n+1}. More precisely, W^n (resp. W^{n+1}) can be written as

$$W^n(x) = \sum_{j=1}^{3} W_j^n \mathcal{N}_j(x) = \text{constant} + \frac{1}{2|T|}\sum_{j=1}^{3} W_j^n \langle \overrightarrow{n}_j, x\rangle,$$

where $\overrightarrow{n}_j$ is the inward normal opposite to the jth vertex of T. Then, taking $\overrightarrow{n}_j = (\alpha_j, \beta_j)^T$, we decompose W_j^n on an eigenvector basis of $\alpha_j A + \beta_j B$ denoted by $\{r_k^j\}_{k=1,d}$ and we recognize that

$$(t - t_n)\langle W_j^n, r_k^j\rangle\langle \overrightarrow{n}_k, x\rangle r_k^j$$

is precisely a simple wave.

In summary, any function piecewise linear in time and space can be decomposed into the sum of $3 \times d$ simple waves

$$U_\sigma(x,t) = \Big(\frac{t-t_n}{\Delta t}(\alpha^{n+1}x+\beta^{n+1}y) + \frac{t_{n+1}-t}{\Delta t}(\alpha^n x+\beta^n y)\Big)r_\sigma = \Big(\frac{t-t_n}{\Delta t}\varphi^{n+1}(x) + \frac{t_{n+1}-t}{\Delta t}\varphi^n(x)\Big)r_\sigma.$$

Then, following once more [6], it is possible to show that the N-scheme (5.2) is monotone on any simple wave, that is the residual Φ_i^N sent to the node i can be written, for a simple wave, as a linear combination of terms like

$$\sum_{j=1,3}\Big(c_{ij}^k\Big)^{n+1}\Big(\varphi_j^{n+1}-\varphi_i^{n+1}\Big)r_j^k \quad \text{and} \quad \sum_{j=1,3}\Big(c_{ij}^k\Big)^{n}\Big(\varphi_j^{n}-\varphi_i^{n}\Big)r_j^k \tag{5.5}$$

with $c_{ij}^k \geqslant 0$ and $k = 1, d$ and φ_j is the value of φ at the jth vertex of T.

Using the above, we introduce the modified N-scheme as follow. We take a direction (α,β), consider the eigenvectors of $\alpha A + \beta B$, write the residual as

$$\Phi_i^N = \sum_{k=1}^{d}\varphi_i^k r_k, \quad \varphi_i^k = \langle \Phi_i^N, r_k\rangle$$

and modify the scalar residual $\{\varphi_i^k\}_{i=1,3}$ as in Section 4.2.4. We notice that $\sum_{i=1}^3 \varphi_i^k = \langle \Phi, r_k\rangle$.

Following [6], and using relations (5.5), it is possible to show that the modified N-scheme is stable.

In the case of a symmetrizable system, we proceed along the same lines. The only modification is that the scalar products between a state variable W or a residual Φ_i^N with an eigenvector r_k are replaced by the inner product between W (resp. Φ_i^N) and the *left* eigenvector ℓ_k associated to the right eigenvector r_k. In fact, it is known that if A_0 is the symmetrization matrix, $A_0 r_k = \ell_k$, so if we make the change of variable $V = A_0 W$, we come back to the symmetric case.

In the previous description, the choice of the direction (α,β) is arbitrary. Different choices will produce different results and different schemes. However, all our numerical experiments for steady and unsteady problems lead to the conclusion that the quality of the results is independent of the direction (α,β). By quality, we mean the non-oscillatory properties of the schemes, and the mesh resolution of the different features of the solution. In all the numerical experiments we present in this paper for fluid problems, we have chosen the vector (α,β) to be the local flow velocity vector, for symmetry reasons mainly.

5.3. Numerical results

In this section we present results on some classical test cases.

5.3.1. A two-dimensional Riemann problem

The initial data are chosen in order to represent a "2D Sod tube" in the domain $[-1,1]\times[-1,1]$:

$$\begin{cases} \rho = 0.1 & \text{if } x\times y < 0,\ 1 \text{ otherwise,}\\ p = 0.1 & \text{if } x\times y < 0,\ 1 \text{ otherwise,}\end{cases} \tag{5.6}$$

and the velocity (u,v) was set to zero. The solution is computed at time $t = 0.2$ on a structured triangulation where $\Delta x = \Delta y = 0.01$ and the CFL number has been set to 0.9.

The isolines of the density and pressure are shown in Figs. 9 and 10 for the N-scheme and the N-modified scheme. See Fig. 11.

5.3.2. A Mach 3 wind tunnel with a forward facing step

This test case has been extensively studied by Woodward and Collela [11], and is widely present in the literature. The setup of the problem is the following: a right-going Mach 3 uniform flow enters a wind tunnel of 1 unit width and 3 units long. The step is 0.2 units high and is located 0.6 units from the left-hand

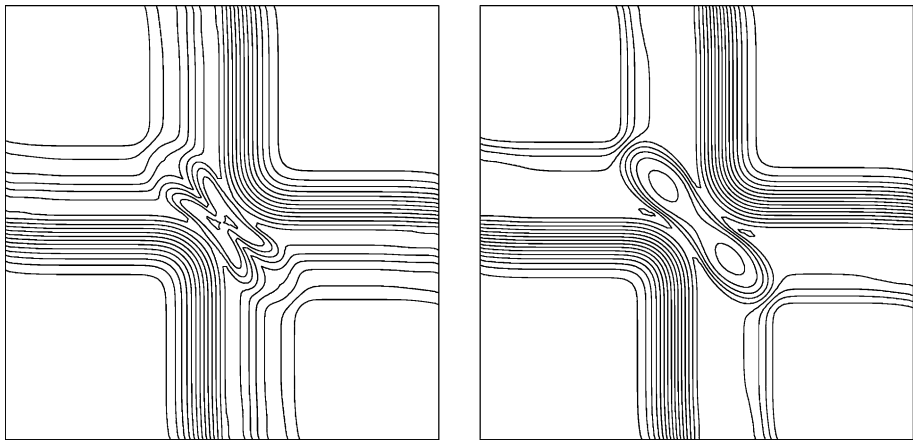

Fig. 9. 2D Riemann problem computed by the N-scheme at time $t = 0.2$: density (left) and pressure (right).

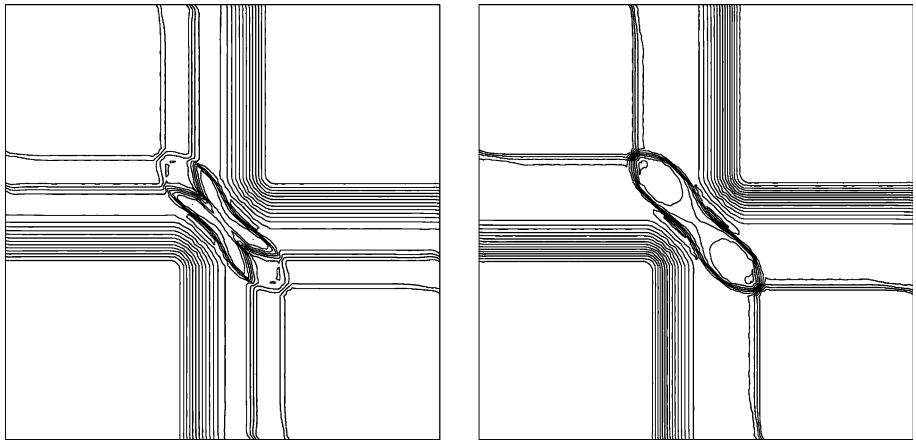

Fig. 10. 2D Riemann problem computed by the N-modified scheme at time $t = 0.2$: density (left) and pressure (right).

end of the tunnel. The problem is initialized by a uniform, right going Mach 3 flow. Reflective boundary conditions are applied along the walls of the tunnel, and inflow and outflow boundary conditions are applied at the entrance and the exit of the tunnel. The results at time $t = 4$ with the N-scheme and the N-modified scheme are shown. The simulation was done at CFL $= 0.9$.

The corner of the step is a singularity. It is well known that if no special treatment is done, an entropy production is observed in the vicinity of the step corner, and it alters the quality of the second reflected shock. This is not physical because we have a strong expansion wave, so no entropy should be created. However, unlike in [11], we do not modify our scheme near the corner, because we are only interested in its stability properties.

An unstructured mesh has been considered, which contains 10,868 nodes and 21,281 triangles, refined near the corner. A portion of the mesh is shown in Fig. 16.

The quality of the slip line coming out of the triple point is noticeable, as well as the resolution of the shocks, in particular at the exit section of the tunnel. The maximum shock width is no larger than two cells.

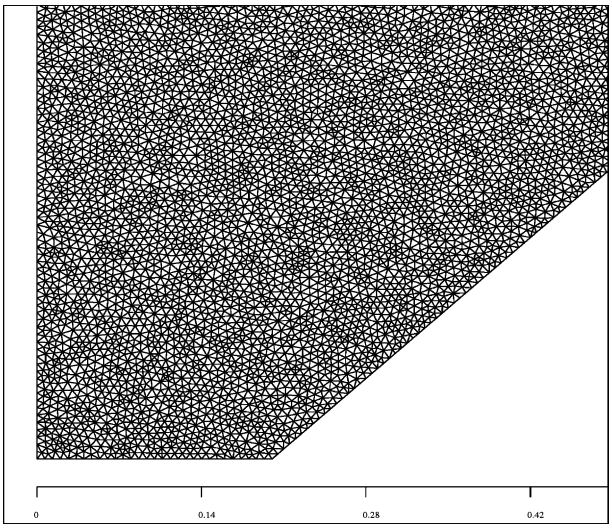

Fig. 11. Part of the unstructured grid.

Between the first order and the second order results, the quality of the fan (at the corner) has dramatically been improved: the reflected shock is now correctly set, the weak compression shock after the fan appears, and interacts with the first reflected shock, see the slip line coming out of the interaction between the reflected shock and the weak compression shock.

5.3.3. Reflection of a shock on a wedge

This problem was studied by Quirk [35]. A planar shock initially enters from the left in a quiescent fluid and is reflected from a 45° ramp. Its Mach number is $M_s = 5.5$ and is defined with respect to the flow values in the quiescent fluid where the density is set to 1.4 and the pressure to 1. Reflective boundary conditions are applied along the ramp and the bottom and the upper of the problem domain. Inflow and outflow boundary conditions are applied at the entrance and the exit of the domain. For this combination of Mach number and ramp angle, a double Mach reflection is expected. The interest of this test case is that, according to [8], the angle $\theta = 45°$ and $M_s = 5.5$ is nearly at the transition between a double Mach reflection and a regular reflection. If the scheme were too diffusive, we would get a regular reflection instead of a double Mach reflection. Hence this is a good test of accuracy.

The density for the N-modified scheme is displayed in Fig. 12. The CFL number has been set to 0.9. The resolution of the different structures is quite clean, despite the poor resolution of the mesh.

5.3.4. Shock–vortex interaction problem

This test case describes the interaction between a stationary shock and a vortex. It was first presented by Pao and Salas [34], and was studied by Meadows et al. [32] with a TVD scheme and by Jiang and Shu [28]. The computational domain is taken to be $[0,2] \times [0,1]$. A stationary Mach 1.1 shock is set at $x = 0.5$ and normal to the x-axis. Its left state is $(\rho, u, v, p) = (1, \sqrt{\gamma}, 0, 1)$. A small vortex is superposed to the flow left of the shock and centered at $(x_c, y_c) = (0.5, 0.25)$. The vortex is described as a perturbation to the velocity (u, v), temperature $T = p/\rho$ and entropy $S = \ln(p/\rho^\gamma)$ of the mean flow and denoted by tilde values

$$\tilde{u} = \epsilon\tau e^{\alpha(1-\tau^2)} \sin\theta, \tag{5.7}$$

$$\tilde{v} = -\epsilon\tau e^{\alpha(1-\tau^2)} \cos\theta, \tag{5.8}$$

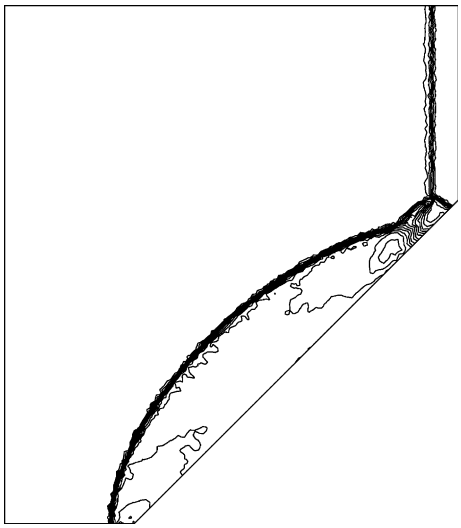

Fig. 12. Reflection of a planar shock from a ramp. Density 20 contour lines from 1.18 to 20.12.

$$\tilde{T} = -\frac{(\gamma-1)\epsilon^2 e^{2\alpha(1-\tau^2)}}{4\alpha\gamma}, \tag{5.9}$$

$$\tilde{S} = 0, \tag{5.10}$$

where $\tau = r/r_c$ and $r = \sqrt{(x-x_c)^2 + (y-y_c)^2}$. Here ϵ indicates the strength of the vortex, α controls the decay rate of the vortex, and r_c is the critical radius for which the vortex has the maximum strength. We choose the same values as in [28], i.e., $\epsilon = 0.3$, $r_c = 0.05$ and $\alpha = 0.204$. The above defined vortex is a steady solution to the 2D Euler equation. The upper and lower boundary are set to be reflective. We use a uniform grid of 251×100, a zoom of which is shown on Fig. 13. The pressure isolines for the N-modified scheme at three different times are displayed in Fig. 14. The CFL number has been set to 0.9.

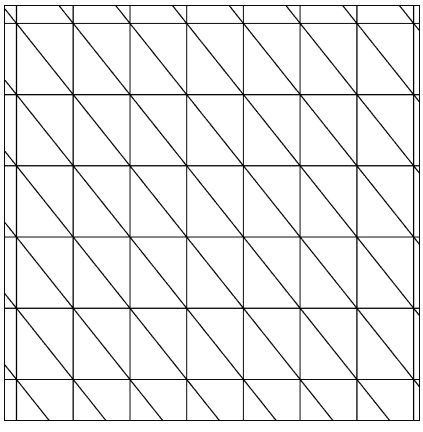

Fig. 13. Zoom of the mesh for the vortex simulation.

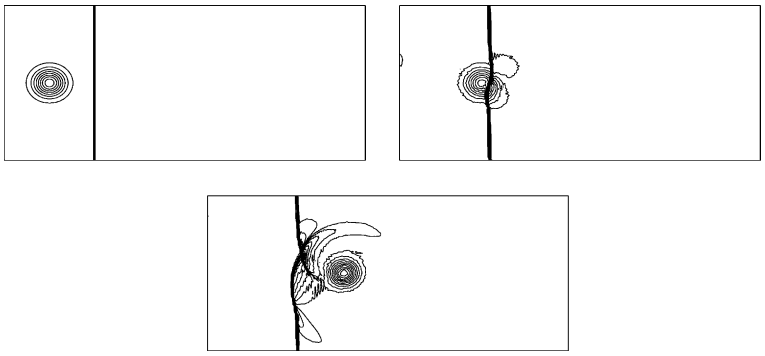

Fig. 14. Shock vortex interaction. Pressure. N-modified scheme: 30 contours lines from 0.84 to 1.4. Top left: $t = 0$; top right: $t = 0.2$, bottom: $t = 0.4$.

6. Toward an unconditionally monotone and LP scheme

In this section we elaborate on an unconditionally monotone and LP scheme, starting from the idea developed in [38], for scalar advection equation and give numerical results for the Euler equations. First we construct an unconditionally monotone scheme, and by limiting contributions we obtain an unconditionally monotone and LP scheme.

Let us consider the scalar advection equation

$$\frac{\partial u}{\partial t} + \langle \overrightarrow{\lambda}, \nabla u \rangle = 0 \quad \text{in } \Omega \times [0, T]. \tag{6.1}$$

The N-scheme reads

$$\Phi_i^N = \frac{|T|}{3}\left(u_i^{n+1} - u_i^n\right) + \frac{\Delta t}{2} \sum_{M_j \in T} k_i^+ N k_j^- \left(u_i^{n+1} - u_j^{n+1} + u_i^n - u_j^n\right). \tag{6.2}$$

It is an upwind scheme in the prismatic element K: no contribution is sent to the past node located at time t_n (upwinding in time).

We have shown that the N-scheme is a monotone scheme under a CFL-like condition. If we write the N-scheme as $Au^{n+1} = Bu^n$, we have shown that A^{-1} has positive elements and B has the same property under a certain condition. In [38], the authors construct space–time residual distribution schemes using a space–time mesh containing three level of nodes and two layers of elements in the temporal direction. The reason is that two layers of elements appear to be the minimum necessary to allow for a scheme to be unconditionally monotone. The space–time elements are tetrahedrons, which induces some complexity in the scheme.

Here we start from the same remark: we use prismatic elements for simplicity and the techniques developed above. We consider three levels of nodes with temporal coordinates t_n, $t_{n+\alpha}$ and t_{n+1}, $\alpha \in [0, 1]$. This delimits two layers of space–time elements. Considering a triangle T, one notes K_1 and K_2 the prisms delimited by T contained in the first and the second layer, with thickness $\Delta t_1 = t_{n+\alpha} - t_n$ and $\Delta t_2 = t_{n+1} - t_{n+\alpha}$ (see Fig. 15).

6.1. Description of an unconditionally monotone scheme

Starting from the space–time N-scheme (4.6), which was made on a single layer of elements, we reformulate it on two layers of elements to allow us an unconditionally stable time marching procedure while maintaining monotonicity both in space and time.

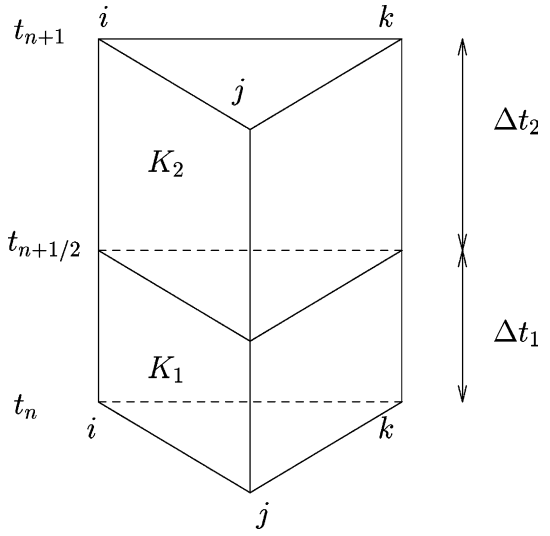

Fig. 15. Space–time grid for the unconditionally monotone and stable scheme.

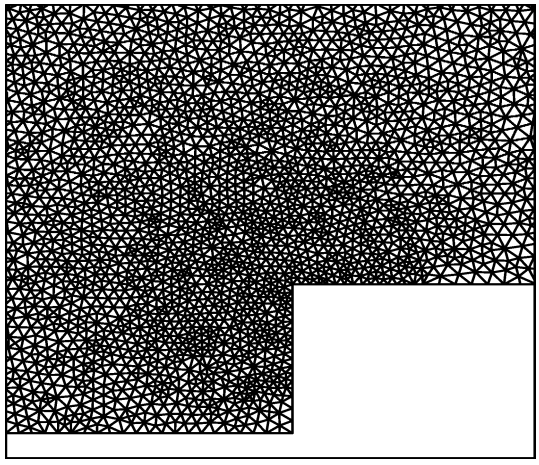

Fig. 16. Part of the unstructured grid for the Mach 3 problem computed with the unconditionally stable scheme.

We denote by $\Phi_{i,n}$, $\Phi_{i,n+\alpha}$ and $\Phi_{i,n+1}$ the residual sent to nodes (M_i, t_n), $(M_i, t_{n+\alpha})$ and (M_i, t_{n+1}). In the first layer, the past does not depend on the future, that is to say $\Phi_{i,n}^{K_1} = 0$. We set

$$\Phi_{i,n+\alpha}^{K_1} = \frac{|T|}{3}\left(u_i^{n+\alpha} - u_i^n\right) + \frac{\Delta t_1}{2}\sum_{M_j \in T} k_i^+ N k_j^- \left(u_i^{n+\alpha} - u_j^{n+\alpha} + u_i^n - u_j^n\right). \tag{6.3}$$

In the second layer we do not impose the upwind property, i.e., $\Phi_{i,n+\alpha}^{K_2} \neq 0$. We set

$$\Phi_{i,n+\alpha}^{K_2} = \frac{\Delta t_2}{2}\sum_{M_j \in T} k_i^+ N k_j^- \left(u_i^{n+\alpha} - u_j^{n+\alpha}\right), \tag{6.4}$$

$$\Phi^{K_2}_{i,n+1} = \frac{|T|}{3}\left(u_i^{n+1} - u_i^{n+\alpha}\right) + \frac{\Delta t_2}{2}\sum_{M_j\in T} k_i^+ N k_j^-\left(u_i^{n+1} - u_j^{n+1}\right), \tag{6.5}$$

Finally the scheme reads

$$\sum_{K,(i,n+\alpha)\in K} \Phi^K_{i,n+\alpha} = 0 \quad \text{and} \quad \sum_{K,(i,n+1)\in K} \Phi^K_{i,n+1} = 0. \tag{6.6}$$

We explain now in detail the contribution to each node.

- For the node$(M_i, t_{n+\alpha})$ one has

$$\Phi^{K_1}_{i,n+\alpha} + \Phi^{K_2}_{i,n+\alpha} = \frac{|T|}{3}\left(u_i^{n+\alpha} - u_i^n\right) + \frac{\Delta t_1}{2}\sum_{M_j\in T} k_i^+ N k_j^-\left(u_i^{n+\alpha} - u_j^{n+\alpha} + u_i^n - u_j^n\right) + \frac{\Delta t_2}{2}\sum_{M_j\in T} k_i^+ N k_j^-\left(u_i^{n+\alpha} - u_j^{n+\alpha}\right), \tag{6.7}$$

$$\Phi^{K_1}_{i,n+\alpha} + \Phi^{K_2}_{i,n+\alpha} = \frac{|T|}{3}\left(u_i^{n+\alpha} - u_i^n\right) + \frac{\Delta t_1}{2}\left(1 + \frac{\Delta t_2}{\Delta t_1}\right)\sum_{M_j\in T} k_i^+ N k_j^-\left(u_i^{n+\alpha} - u_j^{n+\alpha}\right) + \frac{\Delta t_1}{2}\sum_{M_j\in T} k_i^+ N k_j^-\left(u_i^n - u_j^n\right). \tag{6.8}$$

Assembling the contributions of all the elements one obtains $Au^{n+\alpha} = Bu^n$ with

$$A_{ii} = \sum_{T,M_i\in T}\left(\frac{|T|}{3} + \frac{\Delta t_1}{2}\left(1 + \frac{\Delta t_2}{\Delta t_1}\right)k_i^+\right), \quad A_{ij} = \sum_{T,(M_i,M_j)\in T} -\frac{\Delta t_1}{2}\left(1 + \frac{\Delta t_2}{\Delta t_1}\right)k_i^+ N k_j^-, \tag{6.9}$$

$$B_{ii} = \sum_{T,M_i\in T}\left(\frac{|T|}{3} - \frac{\Delta t_1}{2}k_i^+\right), \quad B_{ij} = \sum_{T,(M_i,M_j)\in T}\frac{\Delta t_1}{2}k_i^+ N k_j^-. \tag{6.10}$$

The matrix B has positive entries if Δt_1 satisfies condition (4.10). The inverse of A always exists and has positive entries for all choices of the time steps $\Delta t_1, \Delta t_2$.

- For the node (M_i, t_{n+1}), assembling contributions of all elements gives $Au^{n+1} = Bu^{n+\alpha}$ with

$$A_{ii} = \sum_{T,M_i\in T}\left(\frac{|T|}{3} + \frac{\Delta t_2}{2}k_i^+\right), \quad A_{ij} = \sum_{T,(M_i,M_j)\in T} -\frac{\Delta t_2}{2}k_i^+ N k_j^-, \tag{6.11}$$

$$B_{ii} = \sum_{T,M_i\in T}\frac{|T|}{3}k_i^+, \quad B_{ij} = 0. \tag{6.12}$$

The matrices B and A^{-1} always have positive elements for all choices of time step Δt_2.

The time-step for the first layer (Δt_1) is limited by a CFL-like condition, as we have seen in the previous section for the space–time N-scheme. However, since we do not impose an upwinding condition in time for the second layer, an arbitrary time-step Δt_2 can be chosen. Then the global time-step $\Delta t = \Delta t_1 + \Delta t_2$ is not contrained by any CFL like condition. We have constructed a scheme with unconditionally stable implicit time stepping which maintains full monotonicity.

6.2. An unconditionally monotone and LP scheme

Limiting contributions in the prism K_1 and K_2 gives a monotone and LP scheme. From residuals $\Phi^{K_1}_{i,n+\alpha}$, $\Phi^{K_2}_{i,n+\alpha}$ and $\Phi^{K_2}_{i,n+1}$ we construct modified residuals $\Phi^{K_1*}_{i,n+\alpha}$, $\Phi^{K_2*}_{i,n+\alpha}$ and $\Phi^{K_2*}_{i,n+1}$ in the same way as before (see Section 4.2.4).

- In the prism K_1, we construct $\Phi^{K_1*}_{i,n+\alpha}$ such that

$$\sum_{M_j\in T}\Phi^{K_1*}_{j,n+\alpha}=\Phi^{K_1}, \tag{6.13}$$

$$\Phi^{K_1*}_{i,n+\alpha}=\mathcal{O}(h^3,\Delta t^3). \tag{6.14}$$

- In the prism K_2, we construct $\Phi^{K_2*}_{i,n+\alpha}$ and $\Phi^{K_2*}_{i,n+1}$ such that

$$\sum_{M_j\in T}\left[\Phi^{K_2*}_{j,n+\alpha}+\Phi^{K_2*}_{j,n+1}\right]=\Phi^{K_2}, \tag{6.15}$$

$$\Phi^{K_2*}_{i,n+\alpha}=\mathcal{O}(h^3)+\mathcal{O}(\Delta t^3), \tag{6.16}$$

$$\Phi^{K_2*}_{i,n+1}=\mathcal{O}(h^3)+\mathcal{O}(\Delta t^3). \tag{6.17}$$

Then the solution is advanced from time t_n to time t_{n+1} by the following procedures:

(1) From t_n to $t_{n+\alpha}$. Compute the state at time $t_{n+\alpha}$ by solving

$$\sum_{T,M_i\in T}\left(\Phi^{K_1^*}_{i,n+\alpha}\right)^T=0. \tag{6.18}$$

This is nothing more than the previous scheme of Section 4.2.4 applied between times t_n and $t_{n+\alpha}$. We get predicted states $Z_j^{n+\alpha},\ j=1,\ldots,n_s$.

(2) Then we evaluate $Z_j^{n+1},\ j=1,\ldots,n_s$ by solving

$$\sum_{T,M_i\in T}\left(\Phi^{K_2*}_{j,n+\alpha}\right)^T+\sum_{T,M_i\in T}\left(\Phi^{K_2*}_{j,n+1}\right)^T=0. \tag{6.19}$$

In Eqs. (6.18) and (6.19), the superscript T refers to residuals evaluated for the triangle T. They are solved by Newton iterations.

With this construction the resulting scheme is second order accurate both in time and space, and unconditionally monotone.

In the system case, we extend the scalar schemes to system schemes in a similar fashion, for both prisms K_1 and K_2, as in Sections 5.2.1 and 5.2.3. For example, the residual (6.3) is replaced by (5.3) and (5.4). Similar things are done for the relations (6.4) and (6.5) with obvious modifications. See Fig. 20.

6.3. A numerical example: the Mach 3 wind tunnel with a forward facing step

We use the same mesh as before (see Section 5.3.2), which is refined near the corner, with a fixed ratio $\Delta t_2/\Delta t_1$ equal to 10. Isolines of density, Mach number and entropy at time $t=4$ are shown. The density,

Mach number and entropy deviation are shown in Fig. 21. The results look very similar to those shown in Figs. 17–19. Hence, the same quality of results can be obtained with an improved efficiency. This is very interesting in the case of very non-uniform grids as here.

7. Comments on the efficiency

In the two schemes we have developed, second order results can be obtained via a nonlinear Newton procedure. If first order results are sought, the scheme is also implicit with a linear implicit phase. How many iterations are needed to reach convergence or a satisfactory level of iterative residual? Here, what we call the iterative residual is, in the scalar case, the maximum of the absolute values of the sum of residuals sent at node M_i. In other words, we are converged if for all M_i,

$$\left| \sum_{T, M_i \in T} \Phi_i \right| \leqslant \epsilon$$

for the conditionally monotone scheme and

$$\left| \sum_{T, M_i \in T} \Phi^{K_1}_{i,n+\alpha} \right| \leqslant \epsilon, \quad \left| \sum_{T, M_i \in T} \Phi^{K_2}_{i,n+\alpha} + \Phi i, n + 1^{K_2} \right| \leqslant \epsilon$$

for the unconditionally monotone scheme. The threshold is $\epsilon = 10^{-10}$ for the first order scheme and $\epsilon = 10^{-4}$ for the second order ones. The reason for these choices is that the first order scheme is energy

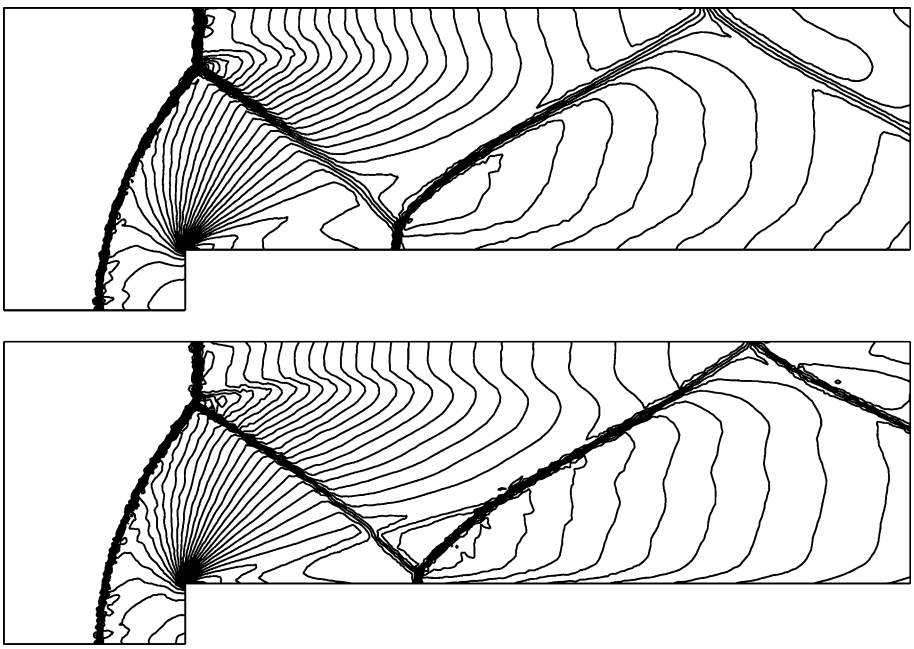

Fig. 17. Forward-facing step problem. Density iso-lines: 30 equally spaced contour lines from 0.09 to 6.23. Top: N scheme; bottom: N-modified scheme.

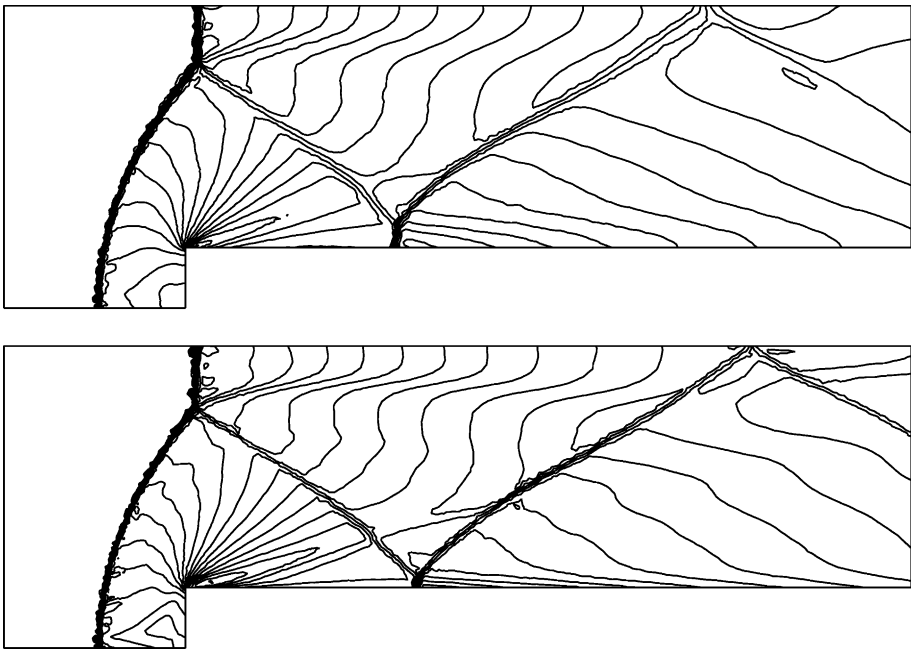

Fig. 18. Forward-facing step problem. Mach number iso-lines: 25 equally spaced contour lines from 0.02 to 3.82. Top: N scheme; bottom: N-modified scheme.

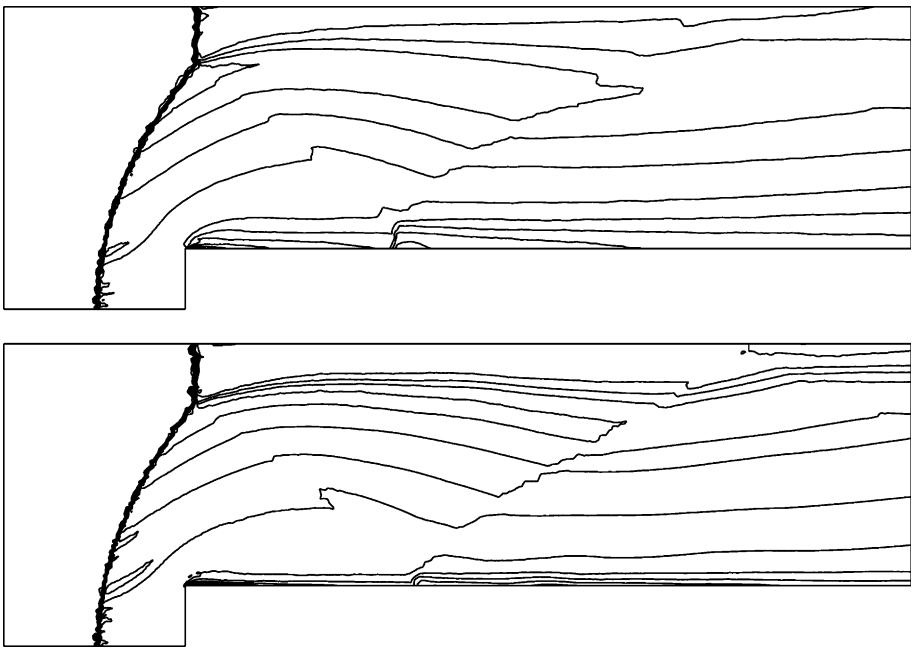

Fig. 19. Forward-facing step problem. Entropy production near the step corner: 17 equally spaced contour lines from 0.63 to 1.5. Top: N scheme; bottom: N-modified scheme.

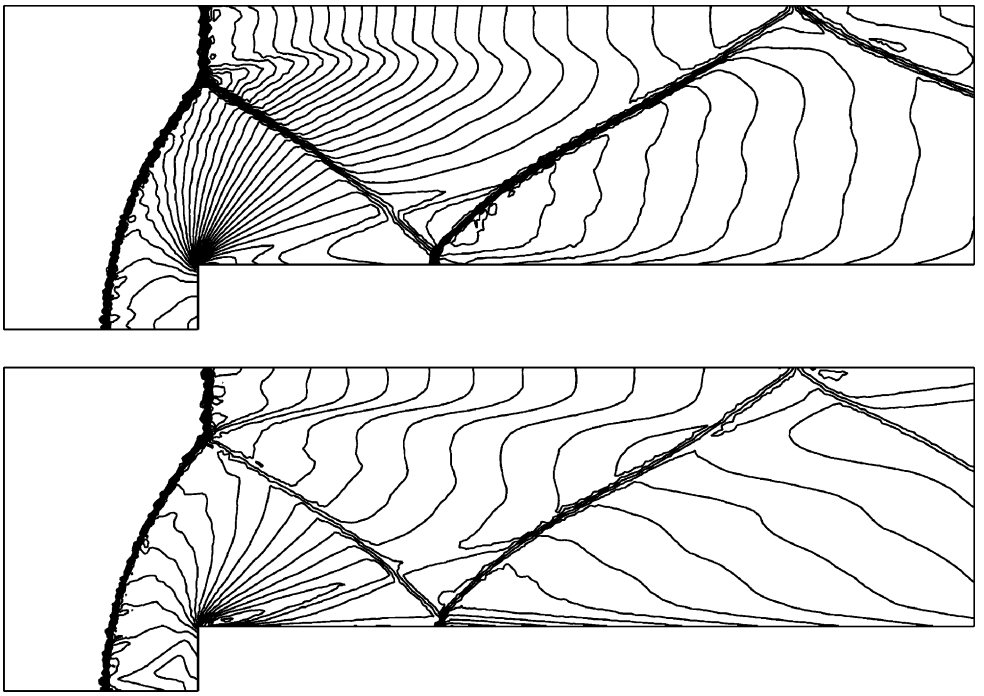

Fig. 20. Forward-facing step problem. Top: density iso-lines: 30 equally spaced contour lines from 0.09 to 6.23. Bottom: Mach number iso-lines: 25 equally spaced contour lines from 0.02 to 3.82. This has been computed with the unconditionally stable N-modified scheme.

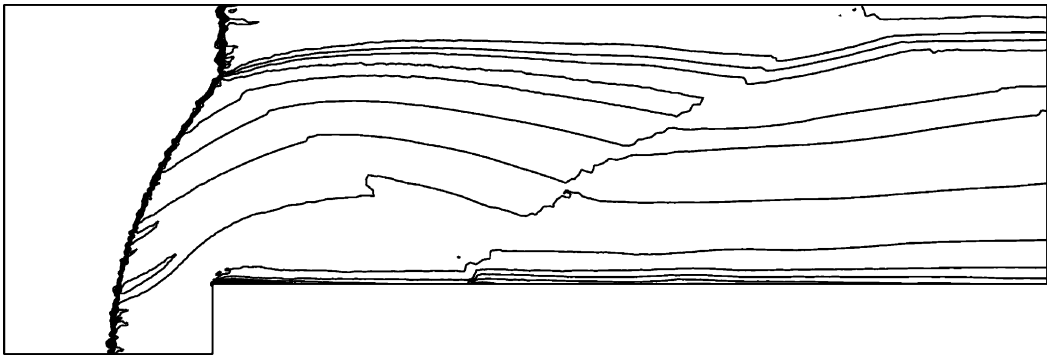

Fig. 21. Forward-facing step problem. Entropy production near the step corner: 17 equally spaced contour lines from 0.63 to 1.5. This has been computed with the unconditionally stable N-modified scheme.

stable so machine zero can be reached, while as usual for residual distribution scheme, we do not know how to reach machine zero for high order residual distribution schemes.

In all our experiments, we needed three to four Newton iterations to reached the prescribed level of iterative convergence.

8. Concluding remarks

We have developed a family of schemes for unsteady flow problems, which have the following characteristics. First they are adapted to unstructured triangular type meshes. The degrees of freedom are located at the vertices of the mesh. They use the most compact stencil for second order accuracy, namely the closest neighbors of a vertex. They are second order accurate in the sense that if the flow is smooth enough, the truncation error is $O(h^2)$, so that the error is formally second order even on irregular meshes. They are upwind, non-oscillatory and parameter free. Lastly, it is possible to make them unconditionally stable without losing their basic properties (monotonicity, upwind and second order accurate).

Our future work will follow two paths. First, how is it possible to introduce viscous terms without loosing the accuracy? A simple splitting is not sufficient, we refer to the work of Lerat and Corre [31]. Second, how is it possible to increase the accuracy of theses scheme? A possibility may be to follow the ideas of [7]: a fourth order scheme for steady scalar problems is introduced which has all the desired properties.

Appendix A. Energy stability of the narrow scheme

This appendix contains the energy stability proof, *without any restriction on the time step* of the narrow scheme for the symmetrizable system

$$\frac{\partial W}{\partial t}+\sum_{i=1}^{2} A_i \frac{\partial W}{\partial x_i}=0, \quad (x,t)\in \mathbb{R}^2\times\mathbb{R}^+, \tag{A.1}$$

where $W\in\mathbb{R}^m$ denotes the vector of conserved variables and the matrices A_i are assumed to be constant. Hence, we assume that there exists a symmetric positive definie matrix A_0 such that via the change of variables $W=A_0V$, the system is

$$\widetilde{A}_0 \frac{\partial V}{\partial t}+\sum_{i=1}^{2} \widetilde{A}_i \frac{\partial V}{\partial x_i}=0, \tag{A.2}$$

where $\widetilde{A}_0$ and the matrices $\widetilde{A}_i=A_iA_0$ are symmetric. The energy norm is defined by

$$\mathscr{E}(W)^2=\frac{1}{2}\sum_T |T| \sum_{M_j\in T}\langle W_j, A_0W_j\rangle.$$

In the following the notation $\tilde{}$ over a matrix will mean that this matrix is symmetric.

The Narrow scheme reads

$$\sum_{T,M_i\in T}\left(\frac{|T|}{3}\left(W_i^{n+1}-W_i^n\right)+\frac{\Delta t}{2}\sum_{M_j\in T}K_i^+NK_j^-\left(W_j^{n+1}-W_i^{n+1}+W_j^n-W_i^n\right)\right)=0. \tag{A.3}$$

In symmetrization variables one has

$$\sum_{T,M_i\in T}\left(\frac{|T|}{3}\widetilde{A}_0\left(V_i^{n+1}-V_i^n\right)+\frac{\Delta t}{2}\sum_{M_j\in T}\widetilde{K}_i^+N\widetilde{K}_j^-\left(V_j^{n+1}-V_i^{n+1}+V_j^n-V_i^n\right)\right)=0. \tag{A.4}$$

We first multiply this equation by $V_i^{n+1} + V_i^n$ to obtain

$$\sum_{M_i\in T}\frac{|T|}{3}\left\langle\widetilde{A}_0\left(V_i^{n+1}-V_i^n\right),V_i^{n+1}+V_i^n\right\rangle+\frac{\Delta t}{2}\sum_{T,M_i\in T}\sum_{M_j\in T}\left\langle\widetilde{K}_i^+N\widetilde{K}_j^-\left(V_j^{n+1}-V_i^{n+1}+V_j^n-V_i^n\right),V_i^{n+1}+V_i^n\right\rangle = 0. \tag{A.5}$$

Summing over the nodes of the mesh we get

$$\sum_{T\in\tau_h}\left(\sum_{M_i\in T}\frac{|T|}{3}\left\langle\widetilde{A}_0\left(V_i^{n+1}-V_i^n\right),V_i^{n+1}+V_i^n\right\rangle+\frac{\Delta t}{2}\sum_{M_i\in T}\sum_{M_j\in T}\left\langle\widetilde{K}_i^+N\widetilde{K}_j^-\left(V_j^{n+1}-V_i^{n+1}+V_j^n-V_i^n\right),V_i^{n+1}+V_i^n\right\rangle\right)=0. \tag{A.6}$$

Using the fact that $\widetilde{A}_0$ is symmetric, one has

$$\begin{aligned}\left\langle\widetilde{A}_0\left(V_i^{n+1}-V_i^n\right),V_i^{n+1}+V_i^n\right\rangle &= \langle\widetilde{A}_0V_i^{n+1},V_i^{n+1}\rangle+\langle\widetilde{A}_0V_i^{n+1},V_i^n\rangle-\langle\widetilde{A}_0V_i^n,V_i^n\rangle-\langle\widetilde{A}_0V_i^n,V_i^{n+1}\rangle\\ &= \langle\widetilde{A}_0V_i^{n+1},V_i^{n+1}\rangle-\langle\widetilde{A}_0V_i^n,V_i^n\rangle.\end{aligned}$$

The second term of (A.6) can be written as

$$\begin{aligned}&\sum_{M_i\in T}\left(\sum_{M_j\in T}\left\langle\widetilde{K}_i^+N\widetilde{K}_j^-\left(V_j^{n+1}-V_i^{n+1}+V_j^n-V_i^n\right),V_i^{n+1}+V_i^n\right\rangle\right)\\ &=\sum_{M_i\in T}\left(\sum_{M_j\in T}\left\langle\widetilde{K}_i^+N\widetilde{K}_j^-\left(V_j^{n+1}+V_j^n\right),V_i^{n+1}+V_i^n\right\rangle-\sum_{M_j\in T}\left\langle\widetilde{K}_i^+N\widetilde{K}_j^-\left(V_i^{n+1}+V_i^n\right),V_i^{n+1}+V_i^n\right\rangle\right)\\ &\quad+\sum_{M_i\in T}\left(\sum_{M_j\neq M_i}\left\langle\widetilde{K}_i^+N\widetilde{K}_j^-\left(V_j^{n+1}+V_j^n\right),V_i^{n+1}+V_i^n\right\rangle+\left\langle\widetilde{K}_i^+\left(V_i^{n+1}+V_i^n\right),V_i^{n+1}+V_i^n\right\rangle\right).\end{aligned}$$

In Eq. (A.6) we can add the term $-\sum_{T\in\tau_h}\sum_{i\in T}\langle\widetilde{K}_i(V_i^{n+1}+V_i^n),V_i^{n+1}+V_i^n\rangle$ because this term is equal to zero since the geometry surrounding a vertex is closed.

$$\begin{aligned}\sum_{T\in\tau_h}\sum_{M_i\in T}\left\langle\widetilde{K}_i\left(V_i^{n+1}+V_i^n\right),V_i^{n+1}+V_i^n\right\rangle &= \sum_{M_i\in\tau_h}\sum_{T,M_i\in T}\left\langle\widetilde{K}_i\left(V_i^{n+1}+V_i^n\right),V_i^{n+1}+V_i^n\right\rangle\\ &= \sum_{M_i\in\tau_h}\left\langle\left(\sum_{T,M_i\in T}\widetilde{K}_i\right)\left(V_i^{n+1}+V_i^n\right),V_i^{n+1}+V_i^n\right\rangle=0.\end{aligned}$$

Eq. (A.6) becomes

$$\sum_{T\in\tau_h}\sum_{M_i\in T}\frac{|T|}{3}\left(\langle\widetilde{A}_0V_i^{n+1},V_i^{n+1}\rangle-\langle\widetilde{A}_0V_i^n,V_i^n\rangle\right)+\frac{\Delta t}{2}\sum_{T\in\tau_h}\sum_{M_i\in T}\left(\frac{1}{2}\langle|\widetilde{K}_i|\left(V_i^{n+1}+V_i^n\right),V_i^{n+1}+V_i^n\rangle+\sum_{M_j\in T}\left\langle\widetilde{K}_i^+N\widetilde{K}_j^-\left(V_j^{n+1}+V_j^n\right),V_i^{n+1}+V_i^n\right\rangle\right)=0. \tag{A.7}$$

Moreover one has

$$\sum_{M_i\in T}\sum_{M_j\in T}\left\langle \widetilde{K}_i^+ N\widetilde{K}_j^-\left(V_j^{n+1}+V_j^n\right),V_i^{n+1}+V_i^n\right\rangle = \sum_{M_i\in T}\sum_{M_j\in T}\left\langle V_j^{n+1}+V_j^n,\widetilde{K}_j^- N\widetilde{K}_i^+\left(V_i^{n+1}+V_i^n\right)\right\rangle$$
$$= \sum_{M_j\in T}\sum_{M_i\in T}\left\langle \widetilde{K}_j^- N\widetilde{K}_i^+\left(V_i^{n+1}+V_i^n\right),V_j^{n+1}+V_j^n\right\rangle.$$

Eq. (A.7) becomes

$$\sum_{T\in\tau_h}\sum_{M_i\in T}\frac{|T|}{3}\left(\langle\widetilde{A}_0V_i^{n+1},V_i^{n+1}\rangle-\langle\widetilde{A}_0V_i^n,V_i^n\rangle\right)+\frac{\Delta t}{2}\sum_{T\in\tau_h}\sum_{M_i\in T}\left(\frac{1}{2}\left\langle|\widetilde{K}_i|\left(V_i^{n+1}+V_i^n\right),V_i^{n+1}+V_i^n\right\rangle\right.$$
$$\left.+\sum_{M_j\in T}\frac{1}{2}\left\langle\widetilde{K}_i^+N\widetilde{K}_j^-\left(V_j^{n+1}+V_j^n\right),V_i^{n+1}+V_i^n\right\rangle+\frac{1}{2}\left\langle\widetilde{K}_i^-N\widetilde{K}_j^+\left(V_j^{n+1}+V_j^n\right),V_i^{n+1}+V_i^n\right\rangle\right)=0. \quad (A.8)$$

Next, rewrite

$$\widetilde{K}_i^+N\widetilde{K}_j^-+\widetilde{K}_i^-N\widetilde{K}_j^+$$

in the following form:

$$K_i^+N\widetilde{K}_j^-+\widetilde{K}_i^-N\widetilde{K}_j^+=\widetilde{K}_iN\widetilde{K}_j+\widetilde{K}_i^+N\widetilde{K}_j^++\widetilde{K}_i^-N\widetilde{K}_j^-,$$

which leads to

$$\sum_{T\in\tau_h}\sum_{M_i\in T}\frac{|T|}{3}\left(\langle\widetilde{A}_0V_i^{n+1},V_i^{n+1}\rangle-\langle\widetilde{A}_0V_i^n,V_i^n\rangle\right)\frac{\Delta t}{2}\sum_{T\in\tau_h}\sum_{M_i\in T}\left(\frac{1}{2}\left\langle\widetilde{K}_iN\widetilde{K}_j\left(V_j^{n+1}+V_j^n\right),V_i^{n+1}+V_i^n\right\rangle\right.$$
$$+\frac{1}{2}\left\langle\widetilde{K}_i^+\left(V_i^{n+1}+V_i^n\right),V_i^{n+1}+V_i^n\right\rangle-\frac{1}{2}\sum_{M_j\in T}\left\langle\widetilde{K}_i^+N\widetilde{K}_j^+\left(V_j^{n+1}+V_j^n\right),V_i^{n+1}+V_i^n\right\rangle$$
$$\left.+\frac{1}{2}\left\langle-\widetilde{K}_i^-\left(V_i^{n+1}+V_i^n\right),V_i^{n+1}+V_i^n\right\rangle+\frac{1}{2}\sum_{M_j\in T}\left\langle\widetilde{K}_i^-N\widetilde{K}_j^-\left(V_j^{n+1}+V_j^n\right),V_i^{n+1}+V_i^n\right\rangle\right)=0. \quad (A.9)$$

Finally one obtains

$$\sum_{T\in\tau_h}\sum_{M_i\in T}\frac{|T|}{3}\left(\left\langle\widetilde{A}_0V_i^{n+1},V_i^{n+1}\right\rangle-\left\langle\widetilde{A}_0V_i^n,V_i^n\right\rangle\right)+\sum_{T\in\tau_h}\left(Q_a^T(V_1,V_2,V_3)+Q_b^T(V_1,V_2,V_3)+Q_{\mathrm{c}}^T(V_1,V_2,V_3)\right)=0. \quad (A.10)$$

In [4], it is shown that Q_a^T, Q_b^T and Q_{c}^T are positive quadratic forms: the system N scheme is energy stable.

References

[1] R. Abgrall, On essentially non-oscillatory schemes on unstructured meshes: analysis and implementation, J. Comp. Phys. 114 (1) (1994) 45–54.
[2] R. Abgrall, Toward the ultimate conservative scheme: following the quest, J. Comp. Phys. 167 (2) (2001) 277–315.
[3] R. Abgrall, T. Barth, Weighted residual distribution schemes for conservation laws via adaptive quadrature, Siam. J. Sci. Comput. (2002), accepted for publication.

[4] R. Abgrall, K. Mer, B. Nkonga, A Lax–Wendroff type theorem for residual schemes, in: M. Haffez, J.J. Chattot (Eds.), Innovative Methods for Numerical Solutions of Partial Differential Equations, World Scientific, Singapore, 2002, pp. 243–266.
[5] R. Abgrall, M. Mezine, A consistent upwind residual scheme for scalar unsteady advection problems, Conference AMIF organized by the European Science Foundation, Tuscany, Italy, October 2000.
[6] R. Abgrall, M. Mezine, Construction of second order accurate monotone and stable residual schemes: the steady case, 2002, submitted. Available from http://www.math.u-bordeaux/~abgrall/Articles/steady.ps.gz.
[7] R. Abgrall, P.L. Roe, Construction of very high order fluctuation scheme, J. Sci. Comput. (2003), accepted. http://www.math.u-bordeaux/~abgrall/Articles/high.ps.gz.
[8] G. Ben-Dor, Shock Wave Reflection Phenomena, Springer, Berlin/New York, 1991.
[9] D. Caraeni, L. Fuchs, Compact third-order multidimensional upwind scheme for Navier Stokes simulations, in: Theoretical and Computational Fluid Dynamics, vol. 15, pp. 373–401, 2002. ISSN 0935–4964.
[10] B. Cockburn, C.-W. Shu, The local discontinuous Galerkin method for time-dependent convection–diffusion systems, SIAM J. Numer. Anal. 35 (6) (1998) 2440–2463 (electronic).
[11] P. Collela, P. Woodward, The numerical simulation of two-dimensionnal fluid with strong shocks, J. Comp. Phys. 54 (1984) 115–173.
[12] À. Csik, M. Riucchiuto, H. Deconinck, S. Poedts, Space–time residual distribution schemes for hyperbolic conservation laws, 15th AIAA Computational Fluid Dynamics Conference, Anahein, CA, USA, AIAA 2001-2617, June 2001.
[13] H. Deconinck, P.L. Roe, R. Struijs, A multidimensional generalisation of Roe's difference splitter for the Euler equations, Comput. Fluids 22 (2/3) (1993) 215–222.
[14] H. Deconinck, K. Sermeus, R. Abgrall, Status of multidimensional upwind residual distribution schemes and applications in aeronautics, AIAA CFD Conference, Denver (USA), AIAA paper 2000-2328, June 2000.
[15] H. Deconinck, R. Struijs, G. Bourgeois, P.L. Roe, Compact advection schemes on unstructured meshes, VKI Lecture Series 1993-04, Computational Fluid Dynamics, 1993.
[16] H. Deconinck, R. Struijs, G. Bourgeois, P.L. Roe, Compact advection schemes on unstructured meshes. VKI Lecture Series 1993-04, Computational Fluid Dynamics, 1993.
[17] A. Ferrante, Solution of the unsteady Euler equations using residual distribution and flux correcte transport, Technical report, von Kàrman Institute, Chaussée de Waterloo, 72, B-1640 Rhode Saint Genèse, Belgium, 1997 (Project report).
[18] L. Fezoui, B. Stoufflet, A class of implicit upwind schemes for Euler simulations with unstructured meshes, J. Comp. Phys. 84 (1) (1989) 174–206.
[19] O. Friedrich, Weighted essentially non-oscillatory schemes for the interpolation of mean values on unstructured grids, J. Comp. Phys. 144 (1) (1998) 194–212.
[20] E. Godlewski, P.A. Raviart, Hyperbolic systems of conservations laws, I, Ellipse (1991).
[21] E. Godlewski, P.A. Raviart, Hyperbolic systems of conservations laws, II. Applied Mathematical Sciences, Springer, Berlin, 1995.
[22] A. Harten, S. Osher, B. Engquist, S.R. Chakravarthy, Uniformly high-order accurate non-oscillatory schemes iii, J. Comp. Phys. 71 (1987) 231–303.
[23] C. Hu, C.W. Shu, Weighted essentially non-oscillatory schemes on triangular meshes, J. Comp. Phys. 150 (1) (1999) 97–127.
[24] M. Hubbard, P.L. Roe, Compact high resolution algorithms for time dependent advection problems on unstructured grids, Int. J. Numer. Methods Fluids 33 (5) (2000) 711–736.
[25] Th.J.R. Hughes, M. Mallet, A new finite element formulation for computational fluid dynamics. III. The generalized streamline operator for multidimensional advective–diffusive systems, Comput. Methods Appl. Mech. Eng. 58 (1986) 305–328.
[26] Th.J.R. Hughes, M. Mallet, A new finite element formulation for Computational Fluid Dynamics. IV. A discontinuity-capturing operator for multidimensional advective–diffusive systems, Comput. Methods Appl. Mech. Eng. 58 (1986) 329–336.
[27] M.Y. Hussaini, B. van Leer, J. Van Rosendal (Eds.), Upwind and High Resolution Schemes, Springer, Berlin, 1997.
[28] G.-S. Jiang, C.-W. Shu, Efficient implementation of weighted eno schemes, J. Comp. Phys. 126 (1996) 202–228.
[29] C. Johnson, U. Nävert, J. Pitkäranta, Finite element methods for linear hyperbolic problems, Comput. Methods Appl. Mech. Eng. (1984) 285–312.
[30] P. Lascaux, R. Théodor, Analyse numérique matricielle appliquée à l'art de l'ingénieur, Masson, Paris, France, 1986.
[31] A. Lerat, Ch. Corre, A residual-based compact scheme for the compressible Navier–Stokes equations, J. Comp. Phys. 170 (2) (2001) 642–675.
[32] K.R. Meadows, A. Kumar, M.Y. Hussaini, A computational study of the interaction between a vortex and a shock wave, AIAA Paper 89-1043, 1989.
[33] H. Paillère, Multidimensional upwind residual discretisation schemes for the Euler and Navier Stokes equations on unstructured meshes, Ph.D. Thesis, Université Libre de Bruxelles, 1995.
[34] S.P. Pao, M.D. Salas, AIAA Paper 81-1205, 1981.

[35] J.J. Quirk, A contribution to the great Riemann solver debate, Int. J. Numer. Methods Fluids 18 (555–574) (1994).
[36] P.L. Roe, D. Sidilkover, Optimum positive linear schemes for advection in two and three dimensions, SIAM J. Numer. Anal. 29 (6) (1992) 1542–1588.
[37] R. Struijs, H. Deconinck, P.L. Roe, Fluctuation splitting schemes for the 2D Euler equations, VKI LS 1991-01, Computational Fluid Dynamics, 1991.
[38] E. van der Weide, H. Deconinck, Positive matrix distribution schemes for hyperbolic systems, in: Computational Fluid Dynamics '96, Wiley, New York, 1996, pp. 747–753.